iScience

CellPress
OPEN ACCESS

Article

Chemical inhibition of phosphatidylcholine biogenesis reveals its role in mitochondrial division

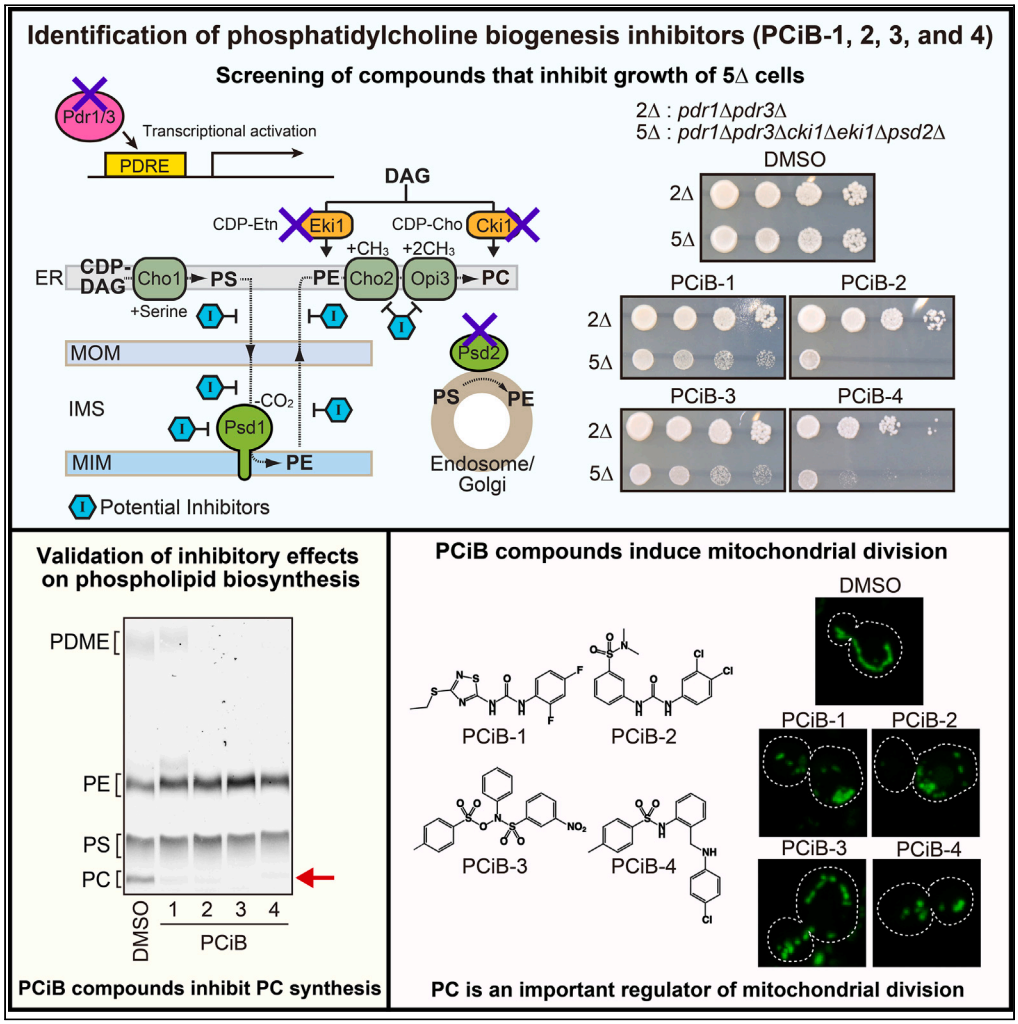

Hiroya Shiino, Shinya Tashiro, Michiko Hashimoto, ..., Toshiya Endo, Hirotatsu Kojima, Yasushi Tamura

tamura@sci.kj.yamagata-u.ac.jp

Highlights

Novel phosphatidylcholine (PC) biogenesis inhibitors (PCiBs) were identified

PCiB-1 is a potential inhibitor of phosphatidylethanolamine (PE) transport

PCiB-2, 3, and 4 inhibit Cho2 PE methyltransferase in yeast

Inhibition of PC biogenesis by PCiB promotes mitochondrial division

Shiino et al., iScience 27, 109189
March 15, 2024
https://doi.org/10.1016/j.isci.2024.109189

iScience

CellPress
OPEN ACCESS

Article

Chemical inhibition of phosphatidylcholine biogenesis reveals its role in mitochondrial division

Hiroya Shiino,[1] Shinya Tashiro,[2] Michiko Hashimoto,[2] Yuki Sakata,[3] Takamitsu Hosoya,[3] Toshiya Endo,[4,5] Hirotatsu Kojima,[6] and Yasushi Tamura[2,7,*]

SUMMARY

Phospholipids are major components of biological membranes and play structural and regulatory roles in various biological processes. To determine the biological significance of phospholipids, the use of chemical inhibitors of phospholipid metabolism offers an effective approach; however, the availability of such compounds is limited. In this study, we performed a chemical–genetic screening using yeast and identified small molecules capable of inhibiting phosphatidylcholine (PC) biogenesis, which we designated PC inhibitors 1, 2, 3, and 4 (PCiB-1, 2, 3, and 4). Biochemical analyses indicated that PCiB-2, 3, and 4 inhibited the phosphatidylethanolamine (PE) methyltransferase activity of Cho2, whereas PCiB-1 may inhibit PE transport from mitochondria to the endoplasmic reticulum (ER). Interestingly, we found that PCiB treatment resulted in mitochondrial fragmentation, which was suppressed by expression of a dominant-negative mutant of the mitochondrial division factor Dnm1. These results provide evidence that normal PC biogenesis is important for the regulation of mitochondrial division.

INTRODUCTION

In yeast, the two most abundant phospholipids, phosphatidylcholine (PC) and phosphatidylethanolamine (PE), are synthesized via phosphatidylserine (PS) decarboxylation and the Kennedy pathway.[1,2] In the first pathway, PS is synthesized in the endoplasmic reticulum (ER) and transferred to mitochondria or the endosome/vacuole, where it is converted to PE by the PS decarboxylases, Psd1 or Psd2.[3] Next, PE is transported from the site of synthesis to the ER, where it is converted to PC by the PE methyltransferases, Cho2, and Opi3.[4–6] Thus, the synthesis of PE and PC relies on the transport of their precursor phospholipids between the ER and mitochondria or endosomal/vacuolar membranes.[3,7–11] The first step in the Kennedy pathway is the conversion of ethanolamine and choline to phosphoethanolamine (P-Etn) and phosphocholine (P-Cho) by Eki1 and Cki1 kinases.[12–14] Next, CDP-Etn and CDP-Cho, which are generated from P-Etn and P-Cho, react with diacylglycerol present in the ER to produce PE and PC, respectively.[15–18] Because Psd1 generates the majority of mitochondrial and cellular PE in yeast,[19,20] the physiological role of Psd1 has been well studied. Loss of Psd1 causes defects in mitochondrial fusion,[21,22] mitochondrial protein trafficking,[23] and the function of mitochondrial respiratory chain proteins,[24–26] which results in impaired respiratory growth. Although PE synthesized outside mitochondria tends to remain in extra-mitochondrial compartments,[20] the enhancement of PE generation by the Kennedy pathway partially rescues the defects caused by Psd1 dysfunction.[25–27] These facts indicate that PE is transported to mitochondria from the outside, although it is inefficient. Psd1 localizes not only to the mitochondrial inner membrane (MIM), but also to the ER membrane. Both have important roles in PE biogenesis in response to metabolic states[28,29]; however, other studies indicate that the role of ER-localized Psd1 is functionally minor.[30,31] These findings indicate that PE synthesis in mitochondria is important for normal mitochondrial function. With respect to PC, previous studies have shown that a decrease in PC results in abnormal mitochondrial protein import and assembly.[32,33] Moreover, the effects of PC depletion on mitochondrial respiratory chain protein stability and membrane potential are lower compared with those associated with PE loss.[25,32] In addition, the involvement of PC in mitochondrial morphogenesis has not been established.

Mitochondria are dynamic membrane structures that constantly fuse and divide to maintain their normal tubular shape, which is important for proper mitochondrial function.[34–36] Dynamin-related GTPase proteins, Fzo1 and Mgm1, facilitate mitochondrial outer membrane (MOM) and MIM fusion, respectively.[37–39] Dnm1, which is also a dynamin-related GTPase, is responsible for mitochondrial division.[40,41] In addition to

[1]Graduate School of Global Symbiotic Sciences, Yamagata University, 1-4-12 Kojirakawa-machi, Yamagata 990-8560, Japan
[2]Faculty of Science, Yamagata University, 1-4-12 Kojirakawa-machi, Yamagata, Yamagata 990-8560, Japan
[3]Laboratory of Chemical Bioscience, Institute of Biomaterials and Bioengineering, Tokyo Medical and Dental University (TMDU), 2-3-10 Kanda-Surugadai, Chiyoda-ku, Tokyo 101-0062, Japan
[4]Faculty of Life Sciences, Kyoto Sangyo University, Kamigamo-motoyama, Kyoto 603-8555, Japan
[5]Institute for Protein Dynamics, Kyoto Sangyo University, Kamigamo-motoyama, Kyoto 603-8555, Japan
[6]Drug Discovery Initiative, Graduate School of Pharmaceutical Sciences, The University of Tokyo, 7-3-1 Hongo, Bunkyo-ku, Tokyo 113-0033, Japan
[7]Lead contact
*Correspondence: tamura@sci.kj.yamagata-u.ac.jp
https://doi.org/10.1016/j.isci.2024.109189

these proteinaceous components of the mitochondrial membrane, phospholipids also play important roles in mitochondrial dynamics. For example, mitochondrial PE and cardiolipin (CL) are necessary for proper mitochondrial fusion.[21,22,42–44] Drp1 (mammalian ortholog of yeast Dnm1) binds directly to CL, which enhances its oligomerization and assembly stimulated GTP hydrolysis to facilitate mitochondrial division.[45–50] In contrast, Drp1 binds to the head group of phosphatidic acid (PA) and saturated acyl chains of another phospholipid in the MOM, thus inhibiting its oligomerization-stimulated GTP hydrolysis.[51]

In the present study, we developed a yeast chemical–genetic screening system to identify compounds that inhibit PC biosynthesis to analyze the physiological significance of PC. Specifically, we screened for small molecules that specifically inhibit the growth of cells lacking Psd2, Eki1, and Cki1. The two predominant phospholipids, PE and PC, are synthesized only via PS decarboxylation in mitochondria and through subsequent PE methylations in the ER in the absence of Psd2, Eki1, and Cki1. Of the compounds that met these criteria, we determined their inhibitory effect on phospholipid metabolism by performing an *in vitro* phospholipid synthesis/transport assay that we previously developed.[52,53] Finally, we selected four compounds that were confirmed to inhibit PC biogenesis, designated PCiB-1, 2, 3, and 4, for *PC i*nhibitors 1, 2, 3, and 4. Our genetic and biochemical analyses revealed that PCiB-1 inhibited the PE transport step from mitochondria to the ER, whereas PCiB-2, 3, and 4 inhibited the phosphatidylethanolamine (PE) methyltransferase activity of Cho2. We also found that mitochondria were markedly fragmented in yeast cells treated with PCiB compounds, which was suppressed following the expression of a dominant-negative mutant of mitochondrial division factor Dnm1.[54] These results indicate that PC biosynthesis is important for the regulation of mitochondrial division.

RESULTS

High-throughput yeast chemical-genetic screen for the identification of phospholipid biogenesis inhibitors

To screen for small molecules that inhibit phospholipid biosynthesis, we generated a yeast mutant strain, in which PE and PC synthesis is highly dependent on the transport of PS and PE between the ER and mitochondria (Figure 1A). We deleted the *EKI1* and *CKI1* genes, which are important for PE and PC synthesis via the Kennedy pathway,[11–13] and the *PSD2* gene,[55] which encodes the extra-mitochondrial PS decarboxylase. In addition, the *PDR1* and *PDR3* genes, which encode transcriptional activators of the multidrug resistance ABC transporters, were deleted to enhance the effect of the small molecule on yeast cells.[56–59] When grown in a normal growth media, in which lyso-PE was not supplemented, the resulting *pdr1Δpdr3Δeki1Δcki1Δpsd2Δ* (termed 5Δ) cells produced PE only through Psd1 in the MIM. In addition, 5Δ cells synthesized PC only by methylation of PE synthesized in mitochondria by ER-resident Cho2 and Opi3 (Figure 1A). The intact PE and PC synthetic pathways in 5Δ cells are considered major pathways in yeast,[18] and we confirmed that control 2Δ (*pdr1Δpdr3Δ*) and 5Δ cells grew similarly (Figure 1B). Thus, we would expect that compounds that exacerbate the growth of the 5Δ, but not the 2Δ strain, would inhibit either PE or PC synthesis step via phospholipid transport between the ER and mitochondria (Figures 1A and 1B). Using over 210,000 compounds provided by the Drug Discovery Initiative at the University of Tokyo, we searched for compounds that inhibited the growth of 5Δ cells. We dispensed 5Δ cell suspensions into 384-well plates and each well contained a different compound. After incubating for 24 h, the OD_{600} was measured as an index of cell growth. Figure 1C shows the representative results from testing 3,200 compounds (10 plates). Among the compounds that strongly inhibited the growth of the 5Δ strain, we selected those that did not inhibit the growth of the 2Δ strain (Figure 1D).

In vitro validation of compound inhibition of phospholipid biosynthesis

To determine whether the compounds identified by cell growth-based screening actually had an inhibitory effect on phospholipid biosynthesis, we used an *in vitro* phospholipid synthesis/transport assay that we developed previously.[52,53] For the *in vitro* assay, we synthesized radioisotope (RI)-labeled PS by incubating a yeast membrane fraction containing the ER and mitochondria with ^{14}C-serine and monitored the conversion of PS to PE and PC. Of the 44 compounds that passed the cell growth-based screening, we identified 7 compounds that significantly inhibited PC synthesis (Figure S1). Because 3 of the 7 compounds were already validated inhibitors, including niguldipine, a calcium channel blocker specific for L-type Cav1.2[60]; bexarotene, a selective retinoid X receptor agonist[61]; and disulfiram, an irreversible inhibitor of aldehyde dehydrogenase,[62] they were excluded from further analysis (Figure S1). We designated the remaining compounds PC inhibitors 1, 2, 3, and 4 (PCiB-1, 2, 3, and 4) and performed further characterizations. PCiB-1 and 2 are structurally similar and both have a phenylurea structure, suggesting that they inhibit the same target molecule. Both PCiB-3 and -4 contain a tosyl group and are structurally different from PCiB-1 and 2 (Figure 2A).

We examined the growth of 2Δ and 5Δ cells on agar plates with or without PCiB-1, 2, 3, and 4 and determined the toxicity against 5Δ cells (Figure 2B). We also carried out the same *in vitro* assay as in Figure S1 and confirmed the specific inhibitory effects of the PCiB compounds on PC synthesis (Figure 2C). PS synthesis was not affected by PCiB compounds (Figure 2C, total), indicating that Cho1 is not their target. Similarly, PE was normally produced and even accumulated in the presence of PCiB compounds (Figures 2C and 3), which indicated that Psd1 activity was unaffected by PCiB. The IC_{50} values of PCiB-1, -2, -3, and -4 against phosphatidyldimethylethanolamine (PDME) and PC synthesis were 7.0, 2.0, 0.4, and 6.8 μM, respectively (Figure 2C).

In vivo validation of PCiB compounds on PC biosynthesis

Since PCiB-1, 2, 3 and 4 showed clear inhibition of PC synthesis *in vitro*, we determined whether they had the same effects *in vivo*. Phospholipids in 2Δ and 5Δ cells were metabolically labeled with ^{32}P-phosphate in the presence or absence of either PCiB compound and analyzed by thin-layer chromatography (TLC). PCiB treatment resulted in similar effects on the phospholipid composition of 2Δ and 5Δ cells. Specifically,

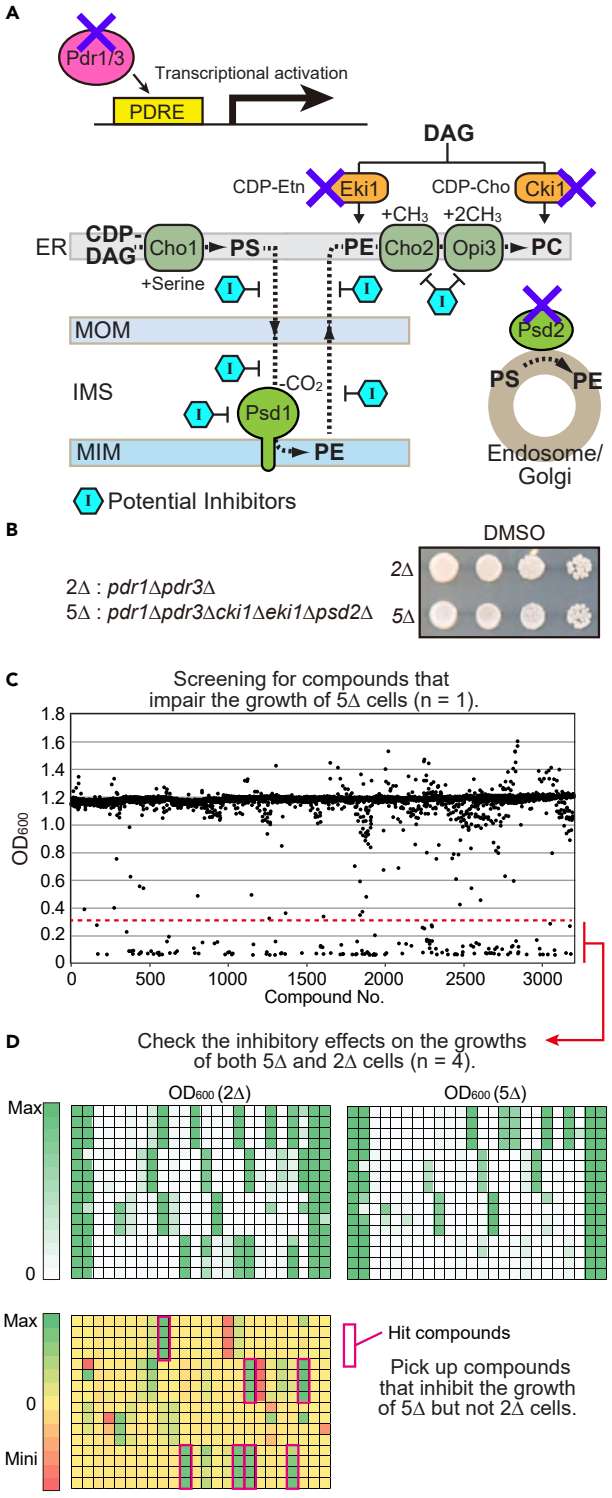

Figure 1. Overview of the chemical–genetic screening to isolate inhibitors of phospholipid biosynthesis

(A) Schematic diagram of 5Δ cells used for the screening. PDRE indicates pleiotropic drug resistance responsive element.

(B) Serial dilutions of 2Δ and 5Δ cells were spotted onto a YPD plate with DMSO and cultivated at 30°C for 2 days.

(C) Of the more than 21,000 compounds screened, results using 3,200 compounds are shown as representative examples.

(D) Compounds that were found to inhibit the growth of 5Δ cells were reexamined for their effect on the growth of 2Δ and 5Δ cells. DMSO was added to two lanes on either end of a 384-well plate. The same compound was added to four vertically adjacent wells.

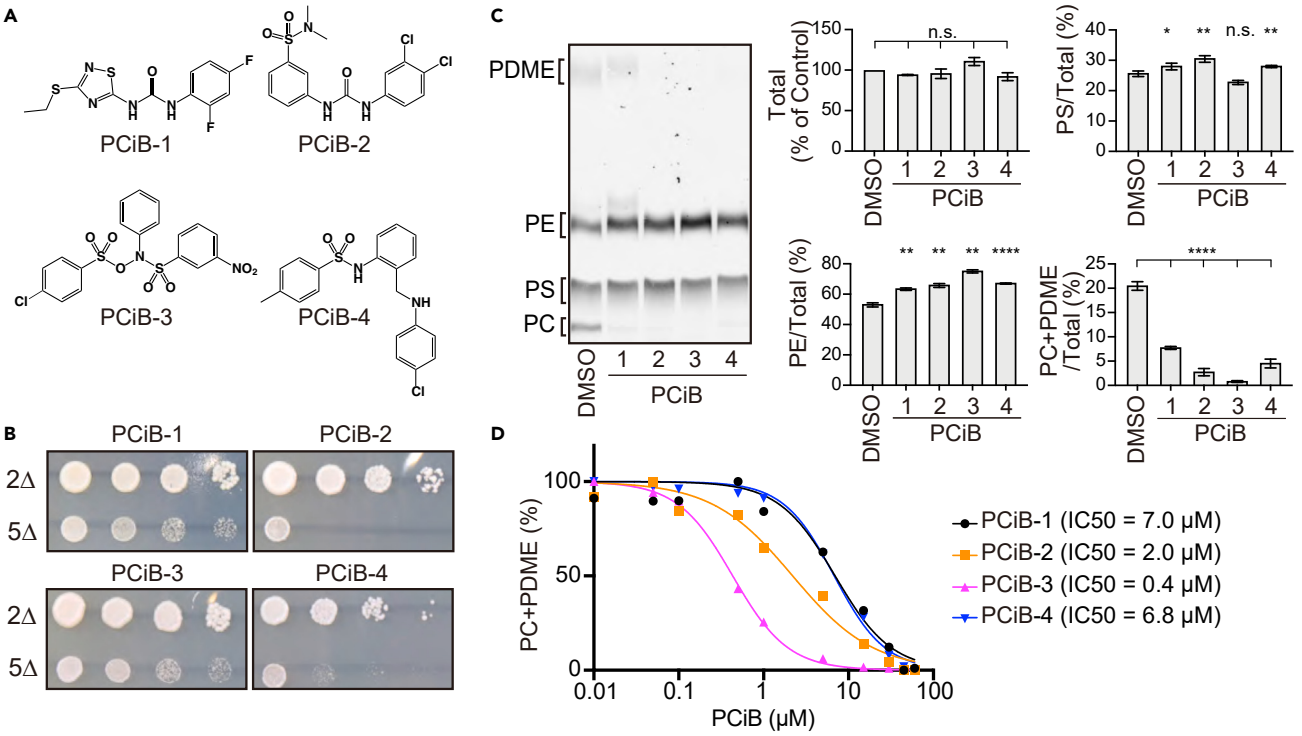

Figure 2. PCiB compounds inhibit the conversion of PE to PC

(A) Chemical structures of PCiB-1, -2, -3, and -4.

(B) Serial dilutions of 2Δ and 5Δ cells were spotted onto a YPD plate with 15 μM PCiB-1, -2, -3, or -4, and cultivated at 30°C for 2 days.

(C) Heavy membrane fractions isolated from wild-type yeast cells were incubated with ^{14}C-Serine for 60 min in the presence of DMSO, PCiB-1, -2, -3, or -4. Phospholipids were extracted and analyzed by TLC followed by radioimaging. The bar graphs indicate the amounts of total ^{14}C-labeled phospholipids relative to DMSO control (100%), and the amounts of PS, PE, and PC + PDME relative to total ^{14}C-labeled phospholipids (100%). Means ± SEM of triplicate experiments were shown. ****p < 0.0001, ***p < 0.001, **p < 0.01, and *p < 0.05; p values were obtained from the unpaired two-tailed t-test.

(D) IC_{50} of PCiB-1, -2, -3, and -4 for the PC + PDME synthesis were measured. The same experiments as in Figure 2C were performed in the presence of different concentration of PCiB-1, -2, -3, or -4 (0.01, 0.05, 0.1, 0.5, 1.0, 5.0, 15, 30, 45, or 60 μM).

PCiB-3 and PCiB-4 markedly inhibited PC synthesis *in vivo*, whereas the inhibitory effects of PCiB-1 and PCiB-2 were weaker than those of PCiB-3 and PCiB-4. (Figures 3A–3C). In addition, a marked accumulation of PE was observed when 2Δ and 5Δ cells were treated with PCiB-3. These results suggest that PCiB-3 inhibits the conversion of PE to PC. We also found that PCiB-2, PCiB-3, and PCiB-4 affected the accumulation of PI differently in 2Δ and 4Δ cells, in which PCiB-2 treatment caused PI accumulation in 2Δ cells, but not in 5Δ cells. Conversely, PCiB-3 treatment resulted in PI accumulation in 5Δ cells, but not in 2Δ cells, whereas PCiB-4 treatment caused PI accumulation in 2Δ and 5Δ cells. As shown in Figures 3E and 3F, the relative amount of PI tended to increase when the synthesis of phospholipids, such as PS, PE, and PC, was inhibited, which indicates that PCiB-2, -3, and -4 affect phospholipid metabolism. We confirmed that the PCiB analogs showed no inhibitory effects on PC accumulation (Figures 3D and S2). These results confirm that PCiB compounds are inhibitors of PC synthesis, although PCiB-1 and -2 were not as effective as PCiB-3 and -4 *in vivo*.

To identify the target molecule of PCiB, we analyzed the phospholipid composition of yeast cells lacking an enzyme involved in PC biosynthesis. Specifically, we metabolically labeled yeast cells lacking either Cho1, Psd1, Cho2, or Opi3 with ^{32}P-phosphate and analyzed the RI-labeled phospholipids by TLC (Figure 3D). As expected, PS and PE levels were decreased relative to total phospholipid levels in *cho1*Δ and *psd1*Δ cells, respectively, whereas the relative levels of PI and PC were increased. These data indicate that along with the *in vitro* results (Figure 2C), Cho1 and Psd1 are unlikely a target of PCiB compounds. On the other hand, relative PC levels were significantly decreased, whereas PE and PI levels were increased in *cho2*Δ cells compared with the wild-type. The phospholipid profile of *cho2*Δ cells was similar to that of PCiB-2, -3 and -4-treated cells (Figures 3B and 3E), suggesting that Cho2 is the target of PCiB compounds. Opi3 is unlikely the target because phosphatidylmonomethylethanolamine (PMME), which is the signature phospholipid of *opi3*Δ cells, did not accumulate in PCiB-treated cells (Figure 3D).

PCiB-2, -3 and -4 impair Cho2 PE methyltransferase activity

Our *in vitro* and *in vivo* analyses suggest that PCiB compounds may inhibit either of the steps involved in the conversion of PE to PC, PE transport from mitochondria to the ER, or PE methylation (Figure 4A). Therefore, we determined whether PCiB compounds block the PE

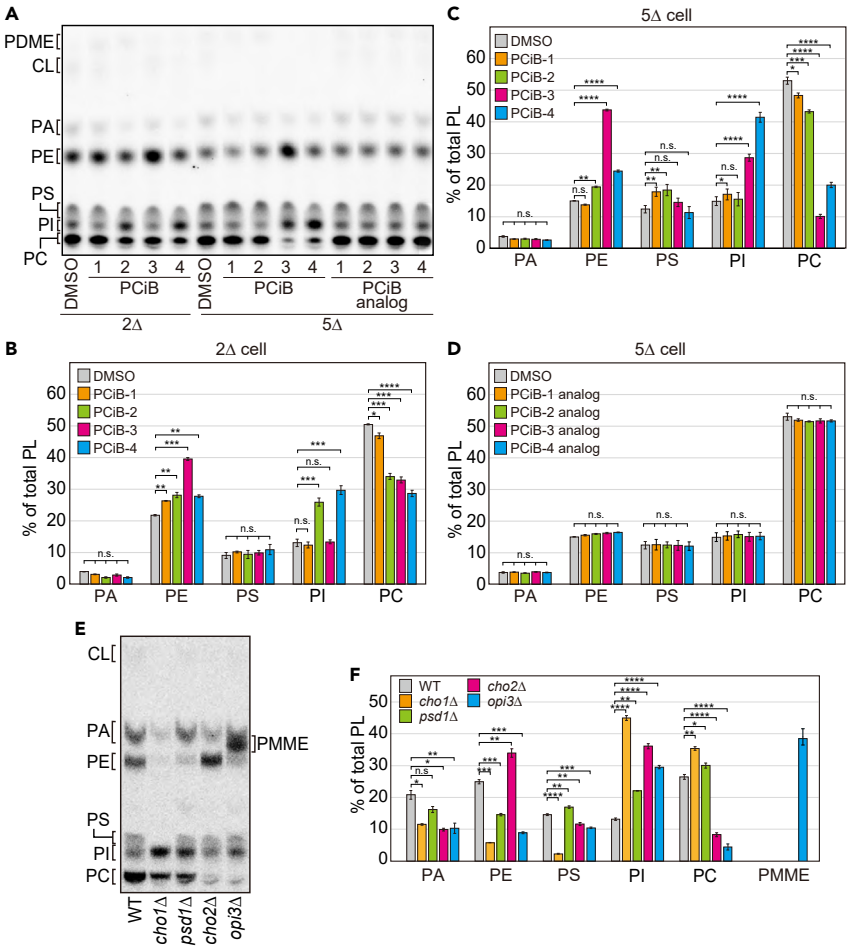

Figure 3. PCiB-3 and -4 affect phospholipid composition *in vivo*

(A) 2Δ and 5Δ cells were cultivated in SCD media containing ^{32}P-phosphate for 6h in the presence of 30 μM PCiB-1, -2, -3, -4, or their analog compound. The total phospholipids were extracted and analyzed by TLC and radioimaging.

(B–D) Amounts of each phospholipid relative to total phospholipids were determined. Values are mean ± SEM (n = 3).

(E) Wild-type, *cho1*Δ, *psd1*Δ, *cho2*Δ, and *opi3*Δ cells were cultivated in SCD media containing ^{32}P-phosphate for 6h. Total phospholipids were extracted from the indicated cells and separated on TLC.

(F) Amounts of each phospholipid relative to total phospholipids were determined. Values are mean ± SEM (n = 3). ****p < 0.0001, ***p < 0.001, **p < 0.01, and *p < 0.05; p values were obtained from the unpaired two-tailed t-test.

methylation step. To directly evaluate PE methylation, we incubated membrane fractions isolated from wild-type or *opi3*Δ cells with ^{3}H-S-adenosylmethionine (SAM), a methyl donor for PE methylation, and measured the synthesis of ^{3}H-labeled PMME, PDME and PC by TLC. Using the wild-type membrane fraction, the amounts of ^{3}H-labeled PMME, PDME, and PC were drastically decreased in the presence of PCiB-2, -3, or -4, whereas they were unchanged following PCiB-1 treatment. These results suggest that PCiB-2, -3, and -4, but not PCiB-1, inhibit Cho2-mediated incorporation of ^{3}H -SAM into PE (Figures 4B and 4C). Similarly, a significant inhibition of ^{3}H-labeled PMME synthesis was observed in the presence of PCiB-2, -3, and -4 using a membrane fraction lacking Opi3, which methylates PMME and PDME.[4,6] These results indicate that Cho2 activity is inhibited in the presence of PCiB-2, -3, and -4. In contrast, PCiB-1 did not have a significant effect on PE methylation (Figures 4B and 4C). Because PCiB-1 clearly inhibits PC synthesis *in vitro* (Figure 2C), PCiB-1 may decelerate PE transport from mitochondria to the ER, resulting in defective PC synthesis. Although it is not known what factors facilitate PE transport from the MIM to MOM, the ERMES complex may be responsible for PE transfer from MOM to the ER.[63–66] Therefore, we determined whether the overexpression of an ERMES subunit (Mmm1, Mdm12, or Mdm34) could rescue the PCiB-associated growth defects. Interestingly, Mmm1, Mdm12, or Mdm34 overexpression largely restored the growth defects of PCiB-1-treated 5Δ cells, whereas it hardly or only slightly restored the growth of PCiB-2 and -4-treated 5Δ cells (Figure 4D). These results suggest that overexpression of a single subunit can improve lipid transport efficiency and promote PC synthesis in the presence of PCiB-1, although the ERMES complex functions as a multi-subunit complex. To confirm this, we evaluated phospholipid transport using membrane fractions overexpressing Mmm1. Immunoblotting of the membrane fraction confirmed that

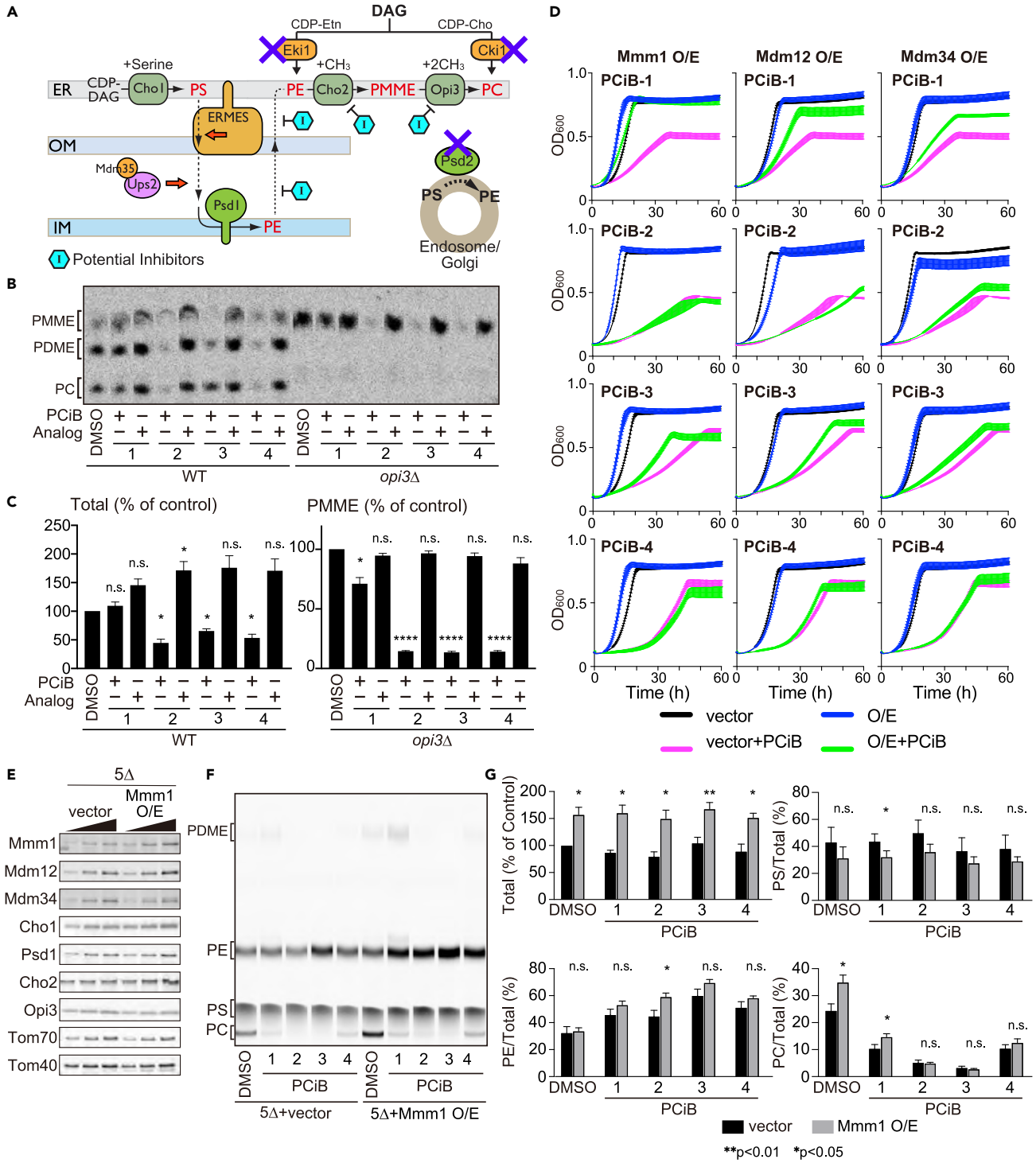

Figure 4. Characterization of PCiB compounds

(A) Schematic diagram of predicted targets of PCiB compounds.

(B) Heavy membrane fractions isolated from wild-type and *opi3*Δ cells were incubated with ^{3}H-SAM for 60 min in the presence of 30 μM PCiB-1, -2, -3, -4, or their analog compounds. The ^{3}H-labeled lipids were analyzed by TLC and autoradiography.

(C) Amounts of total ^{3}H-labeled phospholipid (PMME+PDME+PC) in the wild-type membrane, and amounts of PMME relative to DMSO control in the *opi3*Δ membrane were determined from triplicate experiments. Values are mean ± SEM. (n = 3). ****p < 0.0001, and *p < 0.05; p values were obtained from the unpaired two-tailed t-test.

Figure 4. *Continued*

(D) Proliferation curves are shown for 5Δ cells with the multi-copy plasmid encoding the *MMM1*, *MDM12*, or *MDM34* gene (O/E), or empty vector (vector) in the presence or absence of PCiB compounds. PCiB-1, -3, and -4 were used at 30 μM while PCiB-2 was used at 15 μM. Three independent colonies of 5Δ cells for each condition were cultivated by shaking on a 96-well plate in a plate reader and the OD_{600} values were measured every 20 min for 60 h.

(E) Immunoblotting of membrane fractions isolated from 5Δ cells with the multi-copy plasmid encoding the *MMM1* gene (Mmm1 O/E) or empty vector (vector).

(F) The membrane fractions as in (E) were incubated with ^{14}C-Serine for 60 min in the presence of DMSO, PCiB-1, -2, -3, or -4. Phospholipids were extracted and analyzed by TLC followed by radioimaging.

(G) The bar graphs indicate the amounts of total ^{14}C-labeled phospholipids relative to DMSO control (100%), and the amounts of PS, PE, and PC + PDME relative to total ^{14}C-labeled phospholipids (100%). Values are means ± SEM (n = 4). **p < 0.01, and *p < 0.05; p values were obtained from the unpaired two-tailed t-test.

the amount of Mmm1 was approximately 2-fold higher in 5Δ cells carrying the *2μ*m-plasmid encoding *MMM1* compared with that in the vector control (Figure 4E). The level of an ERMES subunit, Mdm12, and phospholipid synthetic enzymes, Cho1, Psd1, Cho2, and Opi3 were not significantly different upon the Mmm1 overexpression, whereas the level of the ERMES subunit, Mdm34, was slightly decreased (Figure 4E). The MOM proteins, Tom70 and Tom40, were used as loading controls. We performed the *in vitro* phospholipid synthesis/transport assay using the membrane fractions. The results indicated that Mmm1 overexpression significantly enhanced PS synthesis regardless of the presence of PCiB compound (Figures 4F and 4G, total). In addition, we observed that the relative amount of PC was significantly increased in the presence of PCiB-1, but not in the presence of PCiB-2, -3, or -4. These results suggest: 1) overexpression of Mmm1, a single subunit of the ERMES complex, improves the efficiency of phospholipid transport; and 2) Cho1 activity is negatively regulated by PS. Thus, our results likely indicate that PS synthesis is activated by a decrease in the amount of PS in the ER membrane resulting from enhanced PS transport from the ER to mitochondria. We conclude that PCiB-1 likely blocks PE transport from mitochondria to the ER.

PCiB compounds induce mitochondrial division

Because we were able to identify PCiB compounds that inhibit PC biosynthesis, we used them to analyze the physiological significance of PC. In particular, we analyzed the role of PC in mitochondrial morphogenesis, because other phospholipids, such as PE, CL, and PA, regulate mitochondrial fusion and division.[21,22,45–51] We treated 2Δ and 5Δ cells with PCiB compounds and observed mitochondria by fluorescence microscopy. The results indicated that the treatment with PCiB-2, -3, or -4 caused a slight mitochondrial fragmentation in 2Δ cells, whereas the PCiB-1 treatment did not significantly affect mitochondria morphology in 2Δ cells. Moreover, we found that mitochondria were markedly fragmented when 5Δ cells were exposed to any of the compounds (Figures 5A and 5C). The difference in the effect of the PCiB compounds on mitochondrial morphology between 2Δ and 5Δ cells was presumably due to the difference in PE levels. Our phospholipid analysis revealed a relatively higher PE level in 2Δ cells compared with that in 5Δ cells, which was probably due to the presence of Psd2 and/or the Kennedy pathway (Figures 3A–3C). Therefore, we hypothesized that PC plays an important role in mitochondrial morphogenesis and that its significance becomes more pronounced when PE levels are reduced. In support of this concept, we observed that ~60% of *cho2Δ* cells exhibited fragmented mitochondria, while ~40% of the *cho2*Δ cells still maintained tubular mitochondrial morphology (Figures 5B and 5C).

PCiB-1 and PciB-2 markedly fragmented mitochondria in 5Δ cells, despite their low inhibitory effect on PC synthesis *in vivo*. Thus, PCiB-1 and PCiB-2 may exhibit side effects that exacerbate mitochondrial function. Because of the reduction in membrane potential ($\Delta\Psi$) across the MIM, which causes mitochondrial fragmentation,[51,67] we measured the $\Delta\Psi$ of PCiB-treated mitochondria. $\Delta\Psi$ was significantly reduced in the presence of PCiB-1 or PCiB-2, but not PCiB-3 or PCiB-4 (Figure 5D). These results suggest that PCiB-1 and PCiB-2, which have similar structures, share the common effect of decreasing $\Delta\Psi$ and promoting mitochondrial division in a PC-independent manner.

Mitochondrial fragmentation is caused by either increased mitochondrial division or impaired mitochondrial fusion. To distinguish between the two, we observed mitochondria in 5Δ or *cho2*Δ cells expressing Dnm1-109, a dominant-negative mutant that inhibits Dnm1 function.[54,68] Interestingly, most of the 5Δ cells treated with PCiB compounds exhibited elongated tubular mitochondria when Dnm1-109 was expressed. Similarly, we observed connected tubular mitochondria in almost all *cho2*Δ cells expressing Dnm1-109 (Figure 5B). These results clearly indicate that mitochondrial fusion occurs normally in *cho2*Δ cells or PCiB-treated 5Δ cells. Thus, PCiB-induced mitochondrial fragmentation results from enhanced mitochondrial division. In other words, normal PC biogenesis negatively regulates mitochondrial division. To test this idea further, we determined whether the Cho2 overexpression suppresses enhanced mitochondrial division by PCiB-3 and PCiB-4. The results indicated that Cho2 overexpression partly restored mitochondrial tubular morphology in the presence of PCiB-3, but not PCiB-4 (Figures 5E and 5F). These results suggest that PCiB-3 is an inhibitor of Cho2 and that PCiB-4 acts differently from PCiB-3 in inhibiting PC synthesis (Figures 5E and 5F). In support of this, we found that the ER morphology was drastically altered in the presence of PCiB-4, but not PCiB-3 (Fig, 5G). Normally, when labeled the ER membrane with fluorescent proteins, we observe signals from the ER membrane along the plasma membrane and a ring-like signal from the nuclear membrane. 5Δ cells treated with PCiB-3 exhibited a normal ER morphology similar to the DMSO control. In contrast, PCiB-4 treated 5Δ cells displayed a aggregated multiple dot signal. PCiB-1 and PCiB-2 had a minor impact on nuclear morphology (Figure 5G).

When Dnm1 is labeled with a fluorescent protein, oligomerized Dnm1 is detected as multiple punctate signals colocalized with mitochondria[40,69–72]; however, the Dnm1 oligomers exist in a quiescent state and mitochondrial division does not frequently occur at these sites. We also observed that punctate signals of oligomerized Dnm1 were localized to mitochondria in wild-type and *cho2*Δ cells (Figure 5H). The number of Dnm1 dots was slightly larger in *cho2*Δ cells compared with that of the wild-type cells (Figure 5I). Although the increased number of Dnm1 dots may contribute to the enhancement of mitochondrial division, what triggers the initiation of mitochondrial division is still unclear. CL on the MOM activates Dnm1/Drp1 and promotes mitochondrial division,[45–50] whereas Dnm1/Drp1 bound to PA and saturated fatty acids

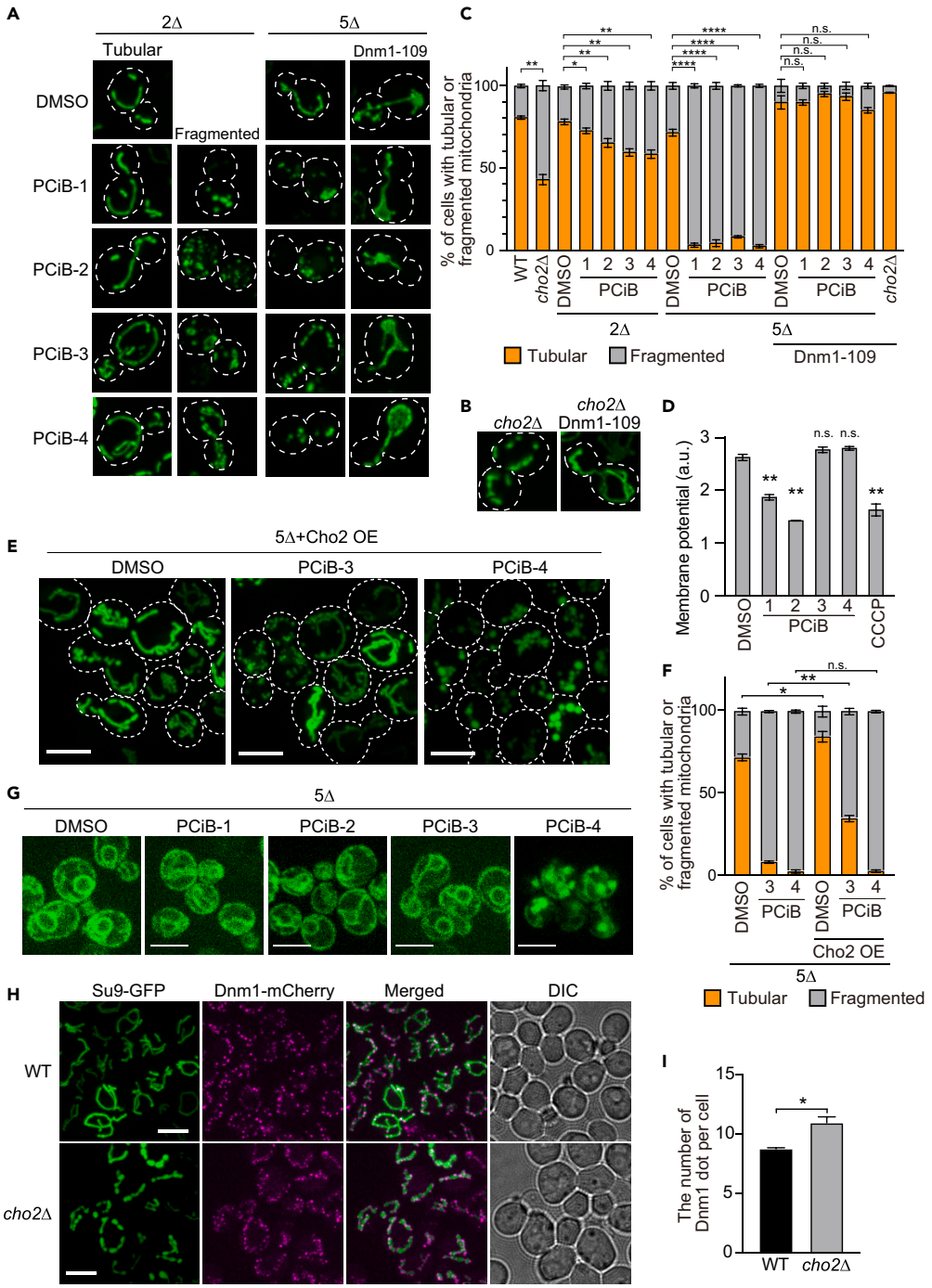

Figure 5. PCiB promotes mitochondrial fragmentation

(A) Mitochondria in 2Δ and 5Δ cells were visualized by expressing mitochondria-targeted GFP (Su9-GFP) and observed under a confocal laser microscope after 6h-incubation with the indicated 30 μM PCiB compound. Mitochondria in 5Δ cells expressing Dnm1-109 (dominant negative mutant) were also observed. Maximum projection images were shown.

(B) Mitochondria in *cho2*Δ cells with or without expression of Dnm1-109 were observed and shown as in (A).

(C) Quantitation of mitochondrial morphology. Cells containing tubular or fragmented mitochondria were scored. Values are mean ± SEM (n = 3). At least 100 cells were visualized in each experiment. ****p < 0.0001, **p < 0.01, and *p < 0.05; p values were obtained from the unpaired two-tailed t-test.

(D) Mitochondrial fraction isolated from wild-type yeast cells were pretreated with the indicated PCiB compound or CCCP and then the ΔΨ was measured by using JC-1 fluorescent dye. Values are mean ± SEM (n = 3). **p < 0.01; p values were obtained from the unpaired two-tailed t-test.

Figure 5. *Continued*

(E) Mitochondria in 5Δ cells overexpressing Cho2 were visualized by Su9-GFP and observed under a confocal laser microscope after 6h-incubation with 30 μM PCiB-3 or -4. Maximum projection images were shown. Scale bars, 5 μm.

(F) The bar graphs show the ratio of cells observed in (E) that contain tubular mitochondria or fragmented mitochondria. Values are mean ± SEM (n = 3). At least 100 cells were visualized in each experiment. **p < 0.01, and *p < 0.05; p values were obtained from the unpaired two-tailed t-test.

(G) The ER in 5Δ cells were visualized by expressing the ER-targeted GFP (BipN-GFP-HDEL) and observed under a confocal laser microscope after 6h-incubation with the indicated 30 μM PCiB compound. A single optical slice around the center of cells is shown for each condition. Scale bars, 5 μm.

(H) Wild-type and *cho2*Δ cells expressing Su9-GFP and Dnm1-mCherry were observed under a confocal laser microscope. Maximum projection images were shown. Scale bars, 5 μm.

(I) The number of punctate Dnm1-mCherry signal per cell was counted. Values are mean ± SEM (n = 3). At least 100 cells were visualized in each experiment. *p < 0.05; p values were obtained from the unpaired two-tailed t-test.

is inactivated.[51] Herein, we found that PC is another important regulator of Dnm1-dependent mitochondrial division, especially when the PE level is low. These findings provide new insight into the regulatory mechanism of mitochondrial division.

DISCUSSION

In the present study, we established a synthetic lethal chemical screen using 5Δ cells, in which the synthesis of PE and PC was strictly dependent on phospholipid transport between the ER and mitochondria (Figure 1A). In principle, the compounds identified using this screen are expected to inhibit multiple steps in the synthesis and transport of PS, PE, and PC. Therefore, we performed a biochemical assay to evaluate their inhibitory effects on phospholipid synthesis and transport. As a result, we identified PCiB compounds that inhibit PC biogenesis in yeast. Specifically, PE methylation was inhibited in the presence of PCiB-2, -3, and -4, whereas PE transport from mitochondria to the ER was presumably blocked by PCiB-1. Because of the similarity in structure between PCiB-1 and -2, it is possible that they act similarly. In other words, the inhibition of PE methylation in the presence of PCiB-2 may be the result of the inhibition of PE export from mitochondria. Although PCiB-3 and PCiB-4 also share similar structural features, they affect phospholipid composition as well as mitochondrial and ER shapes differently, which suggests that they act on PC synthesis through different mechanisms. In any case, future studies are needed to verify the direct interactions between PCiB compounds and their target proteins to validate their targets.

In fungi, there are two PE methyltransferases, Cho2 and Opi3. Cho2 mediates the initial methylation of PE, whereas Opi3 is responsible for the last two methylation steps.[4,6] In higher organisms, such as mammals, only Opi3 is conserved, whereas Cho2 is lost during evolution, suggesting that Cho2 inhibitors may exhibit antifungal activity. In fact, widely used organophosphorus fungicides, such as IBP (*S*-benzyl *O,O*-diisopropyl phosphorothiolate), EDDP (*O*-ethyl *S,S*-diphenyl phosphorodithiolate), and ESBP (*S*-benzyl *O*-ethyl phenylphosphonothiolate) for rice blast control, inhibit PE methylations in *Pyrieularia oryzae*.[73–75] Therefore, PCiB-2, -3, and -4 may also have potential as fungicides against rice blast.

PCiB-1 did not strongly affect PE methylation (Figures 4B and 4C). The growth defect of 5Δ cells induced by PCiB-1 was largely restored by overexpression of a subunit of the ERMES complex, which functions as lipid transfer machinery at the ER-mitochondria contact site (Figure 4D), suggesting that PCiB-1 is an inhibitor of PE transport from mitochondria to the ER. Currently, the factors that facilitate PE transport from the MIM to the MOM are unknown. It is also unclear whether the ERMES complex is responsible for the transport of PE from the MOM to the ER. Previously, we showed that the recombinant Mmm1-Mdm12 complex facilitated nitrobenzoxadiazole (NBD)-PE transport between liposomes,[64] suggesting a role for the ERMES complex in PE transport. However, it was difficult to determine whether the ERMES complex transferred PE because the phospholipid substrate used in this experiment was PE, in which the head group was labeled with NBD.[64] When we evaluated the PE transfer function of ERMES using an *in vitro* assay with membrane fractions and ^{14}C-labeled PE, it was not evident that the ERMES complex was required for PE transport.[52] Furthermore, different studies showed that the Mmm1-Mdm12 complex did not bind to PE at all, although Mmm1 and Mdm12 alone could bind to PE.[65,66] Moreover, the results of our *in vitro* experiments suggest that Mmm1 overexpression promotes PS transport rather than PE transport, which in turn, activated PS synthesis, resulting in the partial restoration of PC synthesis (Figures 4F and 4G). Therefore, PCiB-1 may be used to identify factors involved in the PE transfer process. For example, a multi-copy suppressor screen that restores the growth of 5Δ cells in the presence of PCiB-1 would be a powerful tool for this purpose.

Another important finding of this study is the implication of PC biosynthesis in the regulation of mitochondrial division. CL positively and PA negatively regulate Dnm1/Drp1-dependent mitochondrial division,[44–50] indicating the importance of phospholipids in the regulation of mitochondrial division. The present study further revealed that the inhibition of PC biogenesis promotes mitochondrial division. This suggests that PC serves as a negative regulator of mitochondrial division. Supporting this idea, it has been reported that Drp1 is inactivated by its binding to the head group of PA and the saturated acyl chain of PC.[50] Although steady-state levels of PC varied depending on which PCiB compound was used to treat 5Δ cells, mitochondria were fragmented regardless of the PCiB compound. These results suggest that not only a decrease in PC levels, but also changes in the balance of other phospholipids and/or mitochondrial membrane potential ($\Delta\Psi$) may affect mitochondrial division. In fact, our results strongly suggest that the role of PC in regulating mitochondrial division becomes particularly important under conditions of low PE (Figures 3 and 5). We also found that $\Delta\Psi$ was significantly reduced in the presence of PCiB-1 or -2 (Figure 5D). Although PCiB-3 and PCiB-4 commonly cause marked inhibition of PC synthesis, their effects on mitochondria and ER morphology are different (Figures 5E and 5G), suggesting that they act on different targets. Thus, the amount of PC reduced by PCiB-3 and PCiB-4 may differ depending on the organelle membranes. For example, even if the overall cellular phospholipid compositions do not differ between

PCiB-3- and PCiB-4-treated cells (Figure 3A), the local PC level of certain membranes, such as the MOM and ER membrane, or the ER-mitochondria contact site, may be different. Because mitochondrial division is known to occur at ER-mitochondria contact sites,[76,77] the change in the PC level at the specific region may trigger mitochondrial division. In fact, it was reported that an ER-localized phospholipid hydrolase altered the phospholipid composition at ER-mitochondria sites, which is critical for mitochondrial fusion and division.[78] Collectively, the PCiB compounds obtained in the present study are inhibitors of PC biogenesis in yeast, and they may be used as research tools to analyze the physiological roles of PCs and the mechanisms of mitochondrial morphogenesis.

Limitations of the study

Although we succeeded in isolating several compounds that inhibit PC synthesis in yeast, one limitation of this study is that the targets of PCiB compounds have not been clearly identified. PCiB-2, -3, and -4 strongly inhibit the first PE methylation activity, suggesting that Cho2 is the target of the PCiB compounds. However, PCiB-2, 3, and 4 showed different effects on phospholipid composition (Figures 3 and 4), mitochondrial division (Figure 5), and the ER morphology, suggesting that they have different targets. Specifically, it is unclear at this point why the effect of PI accumulation is different between 2Δ and 5Δ cells treated with PCiB-2 and PCiB-3; why PCiB-1 and -2, but not PCiB-3 and -4, markedly reduce mitochondrial $\Delta\Psi$; why the suppression of mitochondrial division by Cho2 overexpression differs between PCiB-3 and PCiB-4; or why only PCiB-4 results in a drastic change in ER morphology. Furthermore, it has been suggested that PCiB-1 inhibits PE transport, but the transport factors for PE are also unknown. Further studies using these compounds are expected to resolve these issues and contribute to the elucidation of the underlying mechanisms of phospholipid metabolism mediated by the ER and mitochondria.

STAR★METHODS

Detailed methods are provided in the online version of this paper and include the following:

- KEY RESOURCES TABLE
- RESOURCE AVAILABILITY
  - Lead contact
  - Materials availability
  - Data and code availability
- EXPERIMENTAL MODEL AND STUDY PARTICIPANT DETAILS
- METHOD DETAILS
  - Strains, plasmids, primers, and growth conditions
  - Yeast growth based chemical screening
  - *In vitro* phospholipid synthesis/transport assays
  - Immunoblotting
  - Fluorescence microscopy
  - Membrane potential measurement
  - Chemicals
  - Characterization data of compounds
- QUANTIFICATION AND STATISTICAL ANALYSIS

SUPPLEMENTAL INFORMATION

Supplemental information can be found online at https://doi.org/10.1016/j.isci.2024.109189.

ACKNOWLEDGMENTS

We thank Prof. Hiromi Sesaki for the plasmid expressing Dnm1-109. We are grateful to the members of the Tamura and Endo laboratories for helpful discussion. This work was supported by JSPS KAKENHI (Grant Number JP22H02568 to YY, JP15H05705 and JP2222703 to TE), AMED-PRIME (Grant Number JP20gm5910026) from Japan Agency for Medical Research and Development, AMED to YT, Platform Project for Supporting Drug Discovery and Life Science Research (Basis for Supporting Innovative Drug Discovery and Life Science Research (BINDS)) from AMED under Grant Number JP22ama121053 (support number 0178) and JP23ama121043 to T.H. (support number 2768), JST-CREST (Grant Number JPMJCR12M1) and AMED-CREST (Grant Number 21gm1410002), and Takeda Science Foundation grant to TE and YT. HS is a JSPS fellow.

AUTHOR CONTRIBUTIONS

Conceptualization, Y.T.; Methodology, H.S., S.T., M.H., Y.S., T.H., H.K., and Y.T.; Investigation, H.S., S.T., M.H., Y.S., T.H., H.K., and Y.T.; Writing – Original Draft, Y.T.; Writing – Review and Editing, H.S., S.T., Y.S., T.H., T.E., H.K., and Y.T.; Funding Acquisition, H.S., T.H., T.E., H.K., and Y.T.; Resources, T.H., T.E., H.K., and Y.T.; Supervision, T.H., T.E., H.K., and Y.T.

DECLARATION OF INTERESTS

The authors declare that they have no conflict of interest.

DECLARATION OF GENERATIVE AI AND AI-ASSISTED TECHNOLOGIES IN THE WRITING PROCESS

During the preparation of this work the author used ChatGPT in order to check grammatical errors. After using this tool, the author reviewed and edited the content as needed and takes full responsibility for the content of the publication.

Received: October 31, 2023
Revised: December 19, 2023
Accepted: February 6, 2024
Published: February 10, 2024

REFERENCES

1. Di Bartolomeo, F., Wagner, A., and Daum, G. (2017). Cell biology, physiology and enzymology of phosphatidylserine decarboxylase. Biochim. Biophys. Acta. Mol. Cell Biol. Lipids *1862*, 25–38. https://doi.org/10.1016/j.bbalip.2016.09.007.
2. Kwiatek, J.M., Han, G.S., and Carman, G.M. (2020). Phosphatidate-mediated regulation of lipid synthesis at the nuclear/endoplasmic reticulum membrane. Biochim. Biophys. Acta. Mol. Cell Biol. Lipids *1865*, 158434. https://doi.org/10.1016/j.bbalip.2019.03.006.
3. Choi, J.-Y., Riekhof, W.R., Wu, W.-I., and Voelker, D.R. (2006). Macromolecular assemblies regulate nonvesicular phosphatidylserine traffic in yeast. Biochem. Soc. Trans. *34*, 404–408. https://doi.org/10.1042/BST0340404.
4. Kodaki, T., and Yamashita, S. (1987). Yeast phosphatidylethanolamine methylation pathway. Cloning and characterization of two distinct methyltransferase genes. J. Biol. Chem. *262*, 15428–15435.
5. Kanipes, M.I., and Henry, S.A. (1997). The phospholipid methyltransferases in yeast. Biochim. Biophys. Acta *1348*, 134–141. https://doi.org/10.1016/S0005-2760(97)00121-5.
6. McGraw, P., and Henry, S.A. (1989). Mutations in the Saccharomyces cerevisiae opi3 gene: effects on phospholipid methylation, growth and cross-pathway regulation of inositol synthesis. Genetics *122*, 317–330.
7. Tamura, Y., Sesaki, H., and Endo, T. (2014). Phospholipid Transport via Mitochondria. Traffic *15*, 933–945. https://doi.org/10.1111/tra.12188.
8. Dimmer, K.S., and Rapaport, D. (2017). Mitochondrial contact sites as platforms for phospholipid exchange. Biochim. Biophys. Acta. Mol. Cell Biol. Lipids *1862*, 69–80. https://doi.org/10.1016/j.bbalip.2016.07.010.
9. Tatsuta, T., and Langer, T. (2017). Intramitochondrial phospholipid trafficking. Biochim. Biophys. Acta. Mol. Cell Biol. Lipids *1862*, 81–89. https://doi.org/10.1016/j.bbalip.2016.08.006.
10. Riekhof, W., Wu, W., Jones, J., Nikrad, M., Chan, M., Loewen, C., and Voelker, D. (2013). An assembly of proteins and lipid domains regulates transport of phosphatidylserine to phosphatidylserine decarboxylase 2 in Saccharomyces cerevisiae. J. Biol. Chem. *289*, 5809–5819. https://doi.org/10.1074/jbc.M113.518217.
11. Shiino, H., Furuta, S., Kojima, R., Kimura, K., Endo, T., and Tamura, Y. (2021). Phosphatidylserine flux into mitochondria unveiled by organelle-targeted Escherichia coli phosphatidylserine synthase PssA. FEBS J. *288*, 3285–3299. https://doi.org/10.1111/febs.15657.
12. Hosaka, K., Kodaki, T., and Yamashita, S. (1989). Cloning and Characterization of the Yeast CKI Gene Encoding Choline Kinase and Its Expression in Escherichia coli. J. Biol. Chem. *264*, 2053–2059. https://doi.org/10.1016/S0021-9258(18)94140-2.
13. Kim, K.-H., Voelker, D.R., Flocco, M.T., and Carman, G.M. (1998). Expression, Purification, and Characterization of Choline Kinase, Product of the CKI Gene from Saccharomyces cerevisiae. J. Biol. Chem. *273*, 6844–6852. https://doi.org/10.1074/jbc.273.12.6844.
14. Kim, K., Kim, K.-H., Storey, M.K., Voelker, D.R., and Carman, G.M. (1999). Isolation and Characterization of the Saccharomyces cerevisiae EKI1 Gene Encoding Ethanolamine Kinase. J. Biol. Chem. *274*, 14857–14866. https://doi.org/10.1074/jbc.274.21.14857.
15. Tsukagoshi, Y., Nikawa, J., and Yamashita, S. (1987). Molecular cloning and characterization of the gene encoding cholinephosphate cytidylyltransferase in Saccharomyces cerevisiae. Eur. J. Biochem. *169*, 477–486. https://doi.org/10.1111/j.1432-1033.1987.tb13635.x.
16. Min-Seok, R., Kawamata, Y., Nakamura, H., Ohta, A., and Takagi, M. (1996). Isolation and Characterization of ECT1 Gene Encoding CTP: Phosphoethanolamine Cytidylyltransferase of Saccharomyces. J. Biochem. *120*.
17. Hjelmstad, R.H., and Bell, R.M. (1987). Mutants of Saccharomyces cerevisiae defective in sn-1,2-diacylglycerol cholinephosphotransferase. Isolation, characterization, and cloning of the CPT1 gene. J. Biol. Chem. *262*, 3909–3917. https://doi.org/10.1016/S0021-9258(18)61443-7.
18. Hjelmstad, R.H., and Bell, R.M. (1988). The sn-1,2-diacylglycerol ethanolaminephosphotransferase activity of Saccharomyces cerevisiae. Isolation of mutants and cloning of the EPT1 gene. J. Biol. Chem. *263*, 19748–19757.
19. Clancey, C.J., Chang, S.C., and Dowhan, W. (1993). Cloning of a gene (PSD1) encoding phosphatidylserine decarboxylase from Saccharomyces cerevisiae by complementation of an Escherichia coli mutant. J. Biol. Chem. *268*, 24580–24590.
20. Bürgermeister, M., Birner-Grünberger, R., Nebauer, R., and Daum, G. (2004). Contribution of different pathways to the supply of phosphatidylethanolamine and phosphatidylcholine to mitochondrial membranes of the yeast Saccharomyces cerevisiae. Biochim. Biophys. Acta *1686*, 161–168. https://doi.org/10.1016/j.bbalip.2004.09.007.
21. Joshi, A.S., Thompson, M.N., Fei, N., Hüttemann, M., and Greenberg, M.L. (2012). Cardiolipin and mitochondrial phosphatidylethanolamine have overlapping functions in mitochondrial fusion in Saccharomyces cerevisiae. J. Biol. Chem. *287*, 17589–17597. https://doi.org/10.1074/jbc.M111.330167.
22. Chan, E.Y.L., and McQuibban, G.A. (2012). Phosphatidylserine Decarboxylase 1 (Psd1) Promotes Mitochondrial Fusion by Regulating the Biophysical Properties of the Mitochondrial Membrane and Alternative Topogenesis of Mitochondrial Genome Maintenance Protein 1 (Mgm1). J. Biol. Chem. *287*, 40131–40139. https://doi.org/10.1074/jbc.M112.399428.
23. Becker, T., Horvath, S.E., Böttinger, L., Gebert, N., Daum, G., and Pfanner, N. (2013). Role of phosphatidylethanolamine in the biogenesis of mitochondrial outer membrane proteins. J. Biol. Chem. *288*, 16451–16459. https://doi.org/10.1074/jbc.M112.442392.
24. Böttinger, L., Horvath, S.E., Kleinschroth, T., Hunte, C., Daum, G., Pfanner, N., and Becker, T. (2012). Phosphatidylethanolamine and Cardiolipin Differentially Affect the Stability of Mitochondrial Respiratory Chain Supercomplexes. J. Mol. Biol. *423*, 677–686. https://doi.org/10.1016/j.jmb.2012.09.001.
25. Baker, C.D., Basu Ball, W., Pryce, E.N., and Gohil, V.M. (2016). Specific requirements of nonbilayer phospholipids in mitochondrial respiratory chain function and formation. Mol. Biol. Cell *27*, 2161–2171. https://doi.org/10.1091/mbc.E15-12-0865.
26. Calzada, E., Avery, E., Sam, P.N., Modak, A., Wang, C., McCaffery, J.M., Han, X., Alder, N.N., and Claypool, S.M. (2019). Phosphatidylethanolamine made in the inner mitochondrial membrane is essential for yeast cytochrome bc1 complex function. Nat. Commun. *10*, 1432. https://doi.org/10.1038/s41467-019-09425-1.
27. Iadarola, D.M., Basu Ball, W., Trivedi, P.P., Fu, G., Nan, B., and Gohil, V.M. (2020). Vps39 is required for ethanolamine-stimulated elevation in mitochondrial phosphatidylethanolamine. Biochim. Biophys. Acta. Mol. Cell Biol. Lipids *1865*, 158655. https://doi.org/10.1016/j.bbalip.2020.158655.
28. Friedman, J.R., Kannan, M., Toulmay, A., Jan, C.H., Weissman, J.S., Prinz, W.A., and

Nunnari, J. (2018). Lipid Homeostasis Is Maintained by Dual Targeting of the Mitochondrial PE Biosynthesis Enzyme to the ER. Dev. Cell *44*, 261–270. https://doi.org/10.1016/j.devcel.2017.11.023.

29. Gok, M.O., Speer, N.O., Henne, W.M., and Friedman, J.R. (2022). ER-localized phosphatidylethanolamine synthase plays a conserved role in lipid droplet formation. Mol. Biol. Cell *33*, ar11. https://doi.org/10.1091/mbc.E21-11-0558-T.
30. Sam, P.N., Calzada, E., Acoba, M.G., Zhao, T., Watanabe, Y., Nejatfard, A., Trinidad, J.C., Shutt, T.E., Neal, S.E., and Claypool, S.M. (2021). Impaired phosphatidylethanolamine metabolism activates a reversible stress response that detects and resolves mutant mitochondrial precursors. iScience *24*, 102196. https://doi.org/10.1016/j.isci.2021.102196.
31. Kakimoto-Takeda, Y., Kojima, R., Shiino, H., Shinmyo, M., Kurokawa, K., Nakano, A., Endo, T., and Tamura, Y. (2022). Dissociation of ERMES clusters plays a key role in attenuating the endoplasmic reticulum stress. iScience *25*, 105362. https://doi.org/10.1016/j.isci.2022.105362.
32. Schuler, M., Bartolomeo, F.D., Mårtensson, C.U., and Daum, G. (2016). Phosphatidylcholine affects inner membrane protein translocases of mitochondria. J. Biol. Chem. *291*, 18718–18729. https://doi.org/10.1074/jbc.M116.722694.
33. Schuler, M.-H., Di Bartolomeo, F., Böttinger, L., Horvath, S.E., Wenz, L.-S., Daum, G., and Becker, T. (2015). Phosphatidylcholine Affects the Role of the Sorting and Assembly Machinery in the Biogenesis of Mitochondrial β-Barrel Proteins. J. Biol. Chem. *290*, 26523–26532. https://doi.org/10.1074/jbc.M115.687921.
34. Murata, D., Arai, K., Iijima, M., and Sesaki, H. (2020). Mitochondrial division, fusion and degradation. J. Biochem. *167*, 233–241. https://doi.org/10.1093/jb/mvz106.
35. Giacomello, M., Pyakurel, A., Glytsou, C., and Scorrano, L. (2020). The cell biology of mitochondrial membrane dynamics. Nat. Rev. Mol. Cell Biol. *21*, 204–224. https://doi.org/10.1038/s41580-020-0210-7.
36. Tamura, Y., Itoh, K., and Sesaki, H. (2011). SnapShot: Mitochondrial dynamics. Cell *145*, 1158–1158.e1. https://doi.org/10.1016/j.cell.2011.06.018.
37. Rapaport, D., Brunner, M., Neupert, W., and Westermann, B. (1998). Fzo1p is a mitochondrial outer membrane protein essential for the biogenesis of functional mitochondria in Saccharomyces cerevisiae. J. Biol. Chem. *273*, 20150–20155. https://doi.org/10.1074/jbc.273.32.20150.
38. Hermann, G.J., Thatcher, J.W., Mills, J.P., Hales, K.G., Fuller, M.T., Nunnari, J., and Shaw, J.M. (1998). Mitochondrial Fusion in Yeast Requires the Transmembrane GTPase Fzo1p. J. Cell Biol. *143*, 359–373. https://doi.org/10.1083/jcb.143.2.359.
39. Sesaki, H., Southard, S.M., Yaffe, M.P., and Jensen, R.E. (2003). Mgm1p, a Dynamin-related GTPase, Is Essential for Fusion of the Mitochondrial Outer Membrane. Mol. Biol. Cell *14*, 2342–2356. https://doi.org/10.1091/mbc.e02-12-0788.
40. Otsuga, D., Keegan, B.R., Brisch, E., Thatcher, J.W., Hermann, G.J., Bleazard, W., and Shaw, J.M. (1998). The dynamin-related GTPase, Dnm1p, controls mitochondrial morphology in yeast. J. Cell Biol. *143*, 333–349. https://doi.org/10.1083/jcb.143.2.333.
41. Bleazard, W., McCaffery, J.M., King, E.J., Bale, S., Mozdy, A., Tieu, Q., Nunnari, J., and Shaw, J.M. (1999). The dynamin-related GTPase Dnm1 regulates mitochondrial fission in yeast. Nat. Cell Biol. *1*, 298–304. https://doi.org/10.1038/13014.
42. Zhang, Q., Tamura, Y., Roy, M., Adachi, Y., Iijima, M., and Sesaki, H. (2014). Biosynthesis and roles of phospholipids in mitochondrial fusion, division and mitophagy. Cell. Mol. Life Sci. *71*, 3767–3778. https://doi.org/10.1007/s00018-014-1648-6.
43. Kameoka, S., Adachi, Y., Okamoto, K., Iijima, M., and Sesaki, H. (2018). Phosphatidic Acid and Cardiolipin Coordinate Mitochondrial Dynamics. Trends Cell Biol. *28*, 67–76. https://doi.org/10.1016/j.tcb.2017.08.011.
44. Ban, T., Ishihara, T., Kohno, H., Saita, S., Ichimura, A., Maenaka, K., Oka, T., Mihara, K., and Ishihara, N. (2017). Molecular basis of selective mitochondrial fusion by heterotypic action between OPA1 and cardiolipin. Nat. Cell Biol. *19*, 856–863. https://doi.org/10.1038/ncb3560.
45. Francy, C.A., Clinton, R.W., Fröhlich, C., Murphy, C., and Mears, J.A. (2017). Cryo-EM Studies of Drp1 Reveal Cardiolipin Interactions that Activate the Helical Oligomer. Sci. Rep. *7*, 10744. https://doi.org/10.1038/s41598-017-11008-3.
46. Francy, C.A., Alvarez, F.J.D., Zhou, L., Ramachandran, R., and Mears, J.A. (2015). The Mechanoenzymatic Core of Dynamin-related Protein 1 Comprises the Minimal Machinery Required for Membrane Constriction. J. Biol. Chem. *290*, 11692–11703. https://doi.org/10.1074/jbc.M114.610881.
47. Ugarte-Uribe, B., Müller, H.M., Otsuki, M., Nickel, W., and García-Sáez, A.J. (2014). Dynamin-related Protein 1 (Drp1) Promotes Structural Intermediates of Membrane Division. J. Biol. Chem. *289*, 30645–30656. https://doi.org/10.1074/jbc.M114.575779.
48. Macdonald, P.J., Stepanyants, N., Mehrotra, N., Mears, J.A., Qi, X., Sesaki, H., and Ramachandran, R. (2014). A dimeric equilibrium intermediate nucleates Drp1 reassembly on mitochondrial membranes for fission. Mol. Biol. Cell *25*, 1905–1915. https://doi.org/10.1091/mbc.e14-02-0728.
49. Stepanyants, N., Macdonald, P.J., Francy, C.A., Mears, J.A., Qi, X., and Ramachandran, R. (2015). Cardiolipin's propensity for phase transition and its reorganization by dynamin-related protein 1 form a basis for mitochondrial membrane fission. Mol. Biol. Cell *26*, 3104–3116. https://doi.org/10.1091/mbc.E15-06-0330.
50. Bustillo-Zabalbeitia, I., Montessuit, S., Raemy, E., Basañez, G., Terrones, O., and Martinou, J.-C. (2014). Specific Interaction with Cardiolipin Triggers Functional Activation of Dynamin-Related Protein 1. PLoS One *9*, e102738. https://doi.org/10.1371/journal.pone.0102738.
51. Adachi, Y., Itoh, K., Yamada, T., Cerveny, K.L., Suzuki, T.L., Macdonald, P., Frohman, M.A., Ramachandran, R., Iijima, M., and Sesaki, H. (2016). Coincident Phosphatidic Acid Interaction Restrains Drp1 in Mitochondrial Division. Mol. Cell *63*, 1034–1043. https://doi.org/10.1016/j.molcel.2016.08.013.
52. Kojima, R., Endo, T., and Tamura, Y. (2016). A phospholipid transfer function of ER-mitochondria encounter structure revealed in vitro. Sci. Rep. *6*, 30777. https://doi.org/10.1038/srep30777.
53. Tamura, Y., Kojima, R., and Endo, T. (2019). Advanced In Vitro Assay System to Measure Phosphatidylserine and Phosphatidylethanolamine Transport at ER/Mitochondria Interface. In Encyclopedia of Biophysics, pp. 57–67. https://doi.org/10.1007/978-1-4939-9136-5_6.
54. Sesaki, H., and Jensen, R.E. (1999). Division versus Fusion: Dnm1p and Fzo1p Antagonistically Regulate Mitochondrial Shape. J. Cell Biol. *147*, 699–706. https://doi.org/10.1083/jcb.147.4.699.
55. Trotter, P.J., and Voelker, D.R. (1995). Identification of a non-mitochondrial phosphatidylserine decarboxylase activity (PSD2) in the yeast Saccharomyces cerevisiae. J. Biol. Chem. *270*, 6062–6070. https://doi.org/10.1074/jbc.270.11.6062.
56. Balzi, E., Chen, W., Ulaszewski, S., Capieaux, E., and Goffeau, A. (1987). The multidrug resistance gene PDR1 from Saccharomyces cerevisiae. J. Biol. Chem. *262*, 16871–16879. https://doi.org/10.1016/S0021-9258(18)45464-6.
57. Delaveau, T., Delahodde, A., Carvajal, E., Subik, J., and Jacq, C. (1994). PDR3, a new yeast regulatory gene, is homologous toPDR1 and controls the multidrug resistance phenomenon. Mol. Gen. Genet. *244*, 501–511. https://doi.org/10.1007/BF00583901.
58. Cassidy-Stone, A., Chipuk, J.E., Ingerman, E., Song, C., Yoo, C., Kuwana, T., Kurth, M.J., Shaw, J.T., Hinshaw, J.E., Green, D.R., and Nunnari, J. (2008). Chemical Inhibition of the Mitochondrial Division Dynamin Reveals Its Role in Bax/Bak-Dependent Mitochondrial Outer Membrane Permeabilization. Dev. Cell *14*, 193–204. https://doi.org/10.1016/j.devcel.2007.11.019.
59. Hasson, S.A., Damoiseaux, R., Glavin, J.D., Dabir, D.V., Walker, S.S., and Koehler, C.M. (2010). Substrate specificity of the TIM22 mitochondrial import pathway revealed with small molecule inhibitor of protein translocation. Proc. Natl. Acad. Sci. USA *107*, 9578–9583. https://doi.org/10.1073/pnas.0914387107.
60. Fischer, G., Krumpl, G., Mayer, N., Schneider, W., and Raberger, G. (1987). Antihypertensive effects of niguldipine-HCl (B 844-39), a new calcium antagonist in dogs. J. Cardiovasc. Pharmacol. *10*, 268–273. https://doi.org/10.1097/00005344-198709000-00003.
61. Boehm, M.F., Zhang, L., Zhi, L., McClurg, M.R., Berger, E., Wagoner, M., Mais, D.E., Suto, C.M., Davies, J.A., Heyman, R.A., et al. (1995). Design and Synthesis of Potent Retinoid X Receptor Selective Ligands That Induce Apoptosis in Leukemia Cells. J. Med. Chem. *38*, 3146–3155. https://doi.org/10.1021/jm00016a018.
62. Kitson, T.M. (1975). The effect of disulfiram on the aldehyde dehydrogenases of sheep liver. Biochem. J. *151*, 407–412. https://doi.org/10.1042/bj1510407.
63. Kornmann, B., Currie, E., Collins, S.R., Schuldiner, M., Nunnari, J., Weissman, J.S., and Walter, P. (2009). An ER-mitochondria tethering complex revealed by a synthetic biology screen. Science *325*, 477–481. https://doi.org/10.1126/science.1175088.
64. Kawano, S., Tamura, Y., Kojima, R., Bala, S., Asai, E., Michel, A.H., Kornmann, B., Riezman, I., Riezman, H., Sakae, Y., et al. (2018). Structure–function insights into direct lipid transfer between membranes by Mmm1–Mdm12 of ERMES. J. Cell Biol. *217*, 959–974. https://doi.org/10.1083/jcb.201704119.

65. Jeong, H., Park, J., Jun, Y., and Lee, C. (2017). Crystal structures of Mmm1 and Mdm12–Mmm1 reveal mechanistic insight into phospholipid trafficking at ER-mitochondria contact sites. Proc. Natl. Acad. Sci. USA *114*, E9502–E9511. https://doi.org/10.1073/pnas.1715592114.
66. Jeong, H., Park, J., and Lee, C. (2016). Crystal structure of Mdm12 reveals the architecture and dynamic organization of the ERMES complex. EMBO Rep. *17*, 1857–1871. https://doi.org/10.15252/embr.201642706.
67. Li, S., Xu, S., Roelofs, B.A., Boyman, L., Lederer, W.J., Sesaki, H., and Karbowski, M. (2015). Transient assembly of F-actin on the outer mitochondrial membrane contributes to mitochondrial fission. J. Cell Biol. *208*, 109–123. https://doi.org/10.1083/jcb.201404050.
68. Cerveny, K.L., Studer, S.L., Jensen, R.E., and Sesaki, H. (2007). Yeast Mitochondrial Division and Distribution Require the Cortical Num1 Protein. Dev. Cell *12*, 363–375. https://doi.org/10.1016/j.devcel.2007.01.017.
69. Mozdy, A.D., McCaffery, J.M., and Shaw, J.M. (2000). Dnm1p GTPase-mediated mitochondrial fission is a multi-step process requiring the novel integral membrane component Fis1p. J. Cell Biol. *151*, 367–380. https://doi.org/10.1083/jcb.151.2.367.
70. Naylor, K., Ingerman, E., Okreglak, V., Marino, M., Hinshaw, J.E., and Nunnari, J. (2006). Mdv1 interacts with assembled Dnm1 to promote mitochondrial division. J. Biol. Chem. *281*, 2177–2183. https://doi.org/10.1074/jbc.M507943200.
71. Bui, H.T., Karren, M.A., Bhar, D., and Shaw, J.M. (2012). A novel motif in the yeast mitochondrial dynamin Dnm1 is essential for adaptor binding and membrane recruitment. J. Cell Biol. *199*, 613–622. https://doi.org/10.1083/jcb.201207079.
72. Koirala, S., Guo, Q., Kalia, R., Bui, H.T., Eckert, D.M., Frost, A., and Shaw, J.M. (2013). Interchangeable adaptors regulate mitochondrial dynamin assembly for membrane scission. Proc. Natl. Acad. Sci. USA *110*, E1342–E1351. https://doi.org/10.1073/pnas.1300855110.
73. Akatsuka, T., Kodama, O., and Yamada, H. (1977). A novel mode of action of kitazin P in Pyricularia oryzae. Agric. Biol. Chem. *41*, 2111–2112. https://doi.org/10.1271/bbb1961.41.2111.
74. Kodama, O., Yamada, H., and Akatsuka, T. (1979). Mechanisms of action of organophosphorus fungicides. I. Kitazin P, inhibitor of phosphatidylcholine biosynthesis in Pyricularia oryzae. Agric. Biol. Chem. *43*, 1719–1725. https://doi.org/10.1271/bbb1961.43.1719.
75. Kodama, O., Yamashita, K., and Akatsuka, T. (1980). Mechanisms of action of organophosphorus fungicides. II. Edifenphos, inhibitor of phosphatidylcholine biosynthesis in Pyricularia oryzae. Agric. Biol. Chem. *44*, 1015–1021. https://doi.org/10.1271/bbb1961.44.1015.
76. Friedman, J.R., Lackner, L.L., West, M., DiBenedetto, J.R., Nunnari, J., and Voeltz, G.K. (2011). ER Tubules Mark Sites of Mitochondrial Division. Science *334*, 358–362. https://doi.org/10.1126/science.1207385.
77. Abrisch, R.G., Gumbin, S.C., Wisniewski, B.T., Lackner, L.L., and Voeltz, G.K. (2020). Fission and fusion machineries converge at ER contact sites to regulate mitochondrial morphology. J. Cell Biol. *219*, e201911122. https://doi.org/10.1083/jcb.201911122.
78. Nguyen, T.T., and Voeltz, G.K. (2022). An ER phospholipid hydrolase drives ER-associated mitochondrial constriction for fission and fusion. Elife *11*, e84279. https://doi.org/10.7554/eLife.84279.
79. Winston, F., Dollard, C., and Ricupero-Hovasse, S.L. (1995). Construction of a set of convenient Saccharomyces cerevisiae strains that are isogenic to S288C. Yeast *11*, 53–55. https://doi.org/10.1002/yea.320110107.
80. Tamura, Y., Onguka, O., Hobbs, A.E.A., Jensen, R.E., Iijima, M., Claypool, S.M., and Sesaki, H. (2012). Role for two conserved intermembrane space proteins, Ups1p and Up2p, in intra-mitochondrial phospholipid trafficking. J. Biol. Chem. *287*, 15205–15218. https://doi.org/10.1074/jbc.M111.338665.
81. Sakaue, H., Shiota, T., Ishizaka, N., Kawano, S., Tamura, Y., Tan, K.S., Imai, K., Motono, C., Hirokawa, T., Taki, K., et al. (2019). Porin Associates with Tom22 to Regulate the Mitochondrial Protein Gate Assembly. Mol. Cell *73*, 1044–1055. https://doi.org/10.1016/j.molcel.2019.01.003.
82. Kitada, K., Yamaguchi, E., and Arisawa, M. (1995). Cloning of the Candida glabrata TRP1 and HIS3 genes, and construction of their disruptant strains by sequential integrative transformation. Gene *165*, 203–206. https://doi.org/10.1016/0378-1119(95)00552-H.
83. Kakimoto, Y., Tashiro, S., Kojima, R., Morozumi, Y., Endo, T., and Tamura, Y. (2018). Visualizing multiple inter-organelle contact sites using the organelle-targeted split-GFP system. Sci. Rep. *8*, 6175. https://doi.org/10.1038/s41598-018-24466-0.
84. Schneider, C.A., Rasband, W.S., and Eliceiri, K.W. (2012). NIH Image to ImageJ: 25 years of image analysis. Nat. Methods *9*, 671–675. https://doi.org/10.1038/nmeth.2089.
85. Longtine, M.S., Mckenzie, A., III, Demarini, D.J., Shah, N.G., Wach, A., Brachat, A., Philippsen, P., and Pringle, J.R. (1998). Additional modules for versatile and economical PCR-based gene deletion and modification in Saccharomyces cerevisiae. Yeast *14*, 953–961. https://doi.org/10.1002/(SICI)1097-0061(199807)14:10<953::AID-YEA293>3.0.CO;2-U.
86. Christianson, T.W., Sikorski, R.S., Dante, M., Shero, J.H., and Hieter, P. (1992). Multifunctional yeast high-copy-number shuttle vectors. Gene *110*, 119–122.
87. Sook Cho, N., Hoon Kim, Y., Sun Park, M., Hee Kim, E., Kwon Kang, S., and Park, C.m. (2003). Oxidative Cyclization of Dithiobiuret under Basic Conditions and Theoretical Tautomeric Studies of 5-Amino-2,3-dihydro-1,2,4-thiadiazole-3-thione. HETEROCYCLES *60*, 1401. https://doi.org/10.3987/COM-03-9742.
88. Yoshida, S., Misawa, Y., and Hosoya, T. (2014). Formal C–H-Azidation – Based Shortcut to Diazido Building Blocks for the Versatile Preparation of Photoaffinity Labeling Probes. Eur. J. Org. Chem. *2014*, 3991–3995. https://doi.org/10.1002/ejoc.201402516.

STAR★METHODS

KEY RESOURCES TABLE

REAGENT or RESOURCE	SOURCE	IDENTIFIER
Antibodies		
Rabibit polyclonal anti-Mmm1	Endo Lab	N/A
Rabibit polyclonal anti-Mdm34	Endo Lab	N/A
Rabibit polyclonal anti-Mdm12	Endo Lab	N/A
Rabibit polyclonal anti-Tom70	Endo Lab	N/A
Rabibit polyclonal anti-Tom40	Endo Lab	N/A
Rabibit polyclonal anti-Tim23	Endo Lab	N/A
Rabibit polyclonal anti-Cho1	Kojima et al.[52]	N/A
Rabibit polyclonal anti-Psd1	Kojima et al.[52]	N/A
Rabibit polyclonal anti-Cho2	Kojima et al.[52]	N/A
Rabibit polyclonal anti-Opi3	Kojima et al.[52]	N/A
Cy5 AffiniPure Goat Anti-Rabbit IgG (H+L)	Jackson ImmunoResearch Labs	Cat# 111-175-144; RRID:AB_2338013
Bacterial and virus strains		
XL2-blue	N/A	N/A
Chemicals, peptides, and recombinant proteins		
PCiB-1	Asinex	ASN7114421
PCiB-2	Enamine	Z44598158
PCiB-3	Enamine	Z56757277
PCiB-4	Vitas-M	STK089344
Phosphorus-32 ($H^{33}2PO4$)	PerkinElmer Health Sciences, Inc.	NEX053
L-Serine, [^{14}C(U)]	Moravek, Inc.	MC-265
Adenosyl-L-methionine, S-[methyl-^{3}H]-	PerkinElmer Health Sciences, Inc.	NET155
TLC glass plates, silica gel layer, SILGUR C UV254	Macherey-Nagel	810123
PVDF membrane (Immobilon-FL)	Merck-Millipore	Cat# PFL00010
BSA	Nakarai tesque	Cat# 01860-65
CCCP	Sigma-Aldrich	Cat# C2759
JC-1	Thermo Fisher Scientific	Cat# T3168
ATP	Sigma-Aldrich	Cat# A7699
Zymolyase-20T	Nakalai tesque	Cat# 07663-91
Experimental models: Organisms/strains		
FY833- MATa *ura3-52 his3-Δ200 leu2-Δ1 lys2-Δ202 trp1-Δ63*	Winston et al.[79]	N/A
2Δ- MATa *ura3-52 his3-Δ200 leu2-Δ1 lys2-Δ202 trp1-Δ63 pdr1Δ::kanMX4 pdr3Δ::hphMX*	This study	N/A
5Δ- MATa *ura3-52 his3-Δ200 leu2-Δ1 lys2-Δ202 trp1-Δ63 pdr1Δ::hphMX pdr3Δ::natNT2 cki1Δ::CgTRP1 eki1Δ::CgHIS3 psd2Δ::kanMX4*	This study	N/A
cho1Δ- MATa *ura3-52 his3-Δ200 leu2-Δ1 lys2-Δ202 trp1-Δ63 cho1Δ::kanMX4*	Shiino et al.[11]	N/A
psd1Δ- MATa *ura3-52 his3-Δ200 leu2-Δ1 lys2-Δ202 trp1-Δ63 psd1Δ::kanMX4*	Tamura et al.[80]	N/A
cho2Δ- MATa *ura3-52 his3-Δ200 leu2-Δ1 lys2-Δ202 trp1-Δ63 cho2Δ::kanMX4*	This study	N/A
opi3Δ- MATa *ura3-52 his3-Δ200 leu2-Δ1 lys2-Δ202 trp1-Δ63 opi3Δ::kanMX4*	This study	N/A

(*Continued on next page*)

Continued

REAGENT or RESOURCE	SOURCE	IDENTIFIER
Dnm1-mCherry- MATa ura3-52 his3-Δ200 leu2-Δ1 lys2-Δ202 trp1-Δ63 Dnm1-mCherry::kanMX4	This study	N/A
Dnm1-mCherry cho2Δ- MATa ura3-52 his3-Δ200 leu2-Δ1 lys2-Δ202 trp1-Δ63 Dnm1-mCherry::kanMX4 cho2Δ::hphMX	This study	N/A
Oligonucleotides		
See Table S1		
Recombinant DNA		
pBS-kanMX4	Kakimoto-Takeda et al.[31]	N/A
pBS-hphMX	Kakimoto-Takeda et al.[31]	N/A
pBS-natNT2	Sakaue et al.[81]	N/A
pBS-CgHIS3	Kitada et al.[82]	N/A
pBS-CgTRP1	Kitada et al.[82]	N/A
pRS426-Mmm1	This Study	N/A
pRS426-Mdm12	This Study	N/A
pRS426-Mdm34	This Study	N/A
pRS426-Cho2	Kojima et al.[52]	N/A
pRS316-Su9-GFP	Kakimoto et al.[83]	N/A
pRS315-Dnm1-109-HA	Cerveny et al.[68]	N/A
pRS316-BipN-GFP-HDEL	Kakimoto-Takeda et al.[31]	N/A
Software and algorithms		
ImageJ	Schneider et al.[84]	https://imagej.nih.gov/ij/
GraphPad Prism6	GraphPad	https://www.graphpad.com/scientific-software/prism/

RESOURCE AVAILABILITY

Lead contact

Further information and requests for resources and reagents should be directed to and will be fulfilled by the lead contact, Yasushi Tamura, (tamura@sci.kj.yamagata-u.ac.jp).

Materials availability

Plasmids and yeast strains generated in this study are available from the lead contact.

Data and code availability

All data reported in this article will be shared by the lead contact upon request. This paper does not report original code. Any additional information required to reanalyze the data reported in this paper is available from the lead contact upon request.

EXPERIMENTAL MODEL AND STUDY PARTICIPANT DETAILS

In this study, we used a *Saccharomyces cerevisiae* strain, FY833 (MAT*a ura3-52 his3-D200 leu2-D1 lys2-D202 trp1-D63*) as background strains.[79] All the yeast cells used in this study are listed in the key resources table.

METHOD DETAILS

Strains, plasmids, primers, and growth conditions

To obtain 2Δ and 5Δ cells, we deleted the *PDR1, PDR3, CKI1, EKI1, PSD2, OPI3,* and *CHO2* genes by homologous recombination using the appropriate gene cassettes amplified from the plasmids listed in the key resources table.[85] The primer pairs #NU1080/1081, #NU1084/1085, #YU1143/1144, #NU509/510, #NU403/404, #YU1637/1638, #YU1639/164 were used to amplify the gene cassette for the disruption of the *PDR1, PDR3, CKI1, EKI1, PSD2, OPI3,* and *CHO2* genes, respectively (key resources table).

pRS426-Mmm1, pRS426-Mdm12, and pRS426-Mdm34, *URA3-2μ* plasmids that overexpresses Mmm1, Mdm12, and Mdm34, respectively, from the own promoter, was constructed as follows. DNA fragments encoding the *MMM1*, *MDM12*, and *MDM34* genes with own promoter

and terminator were cut from pRS314-Mmm1, pRS314-Mdm12, and pRS314-Mdm34,[80] with BamHI and XhoI and inserted the BamHI/XhoI site of pRS426 vector.[86]

Yeast cells were grown in YPD (1% yeast extract, 2% polypeptone, and 2% glucose), YPLac (1% yeast extract, 2% polypeptone, and 3% lactic acid), and SCD (0.67% yeast nitrogen base without amino acids, 0.5% casamino acid, and 2% glucose), with appropriate amino acids supplements.

To obtain yeast growth curve, we prepared yeast culture as described below. Briefly, 3 independent colonies of 5Δ cells with vector or 2μ-plasmids were inoculated to SCD media and cultivated for 24h. The overnight cultures were diluted with SCD media to OD_{600} = 0.01 and 100 μl aliquots were dispensed to a 96-well plate with or without PCiB compounds. The 96-well plate was incubated at room temperature withdouble orbital shaking at 425 cpm in a plate reader (Epoch 2, BioTek), and the OD_{600} values were measured every 20 min for 60 h.

Yeast growth based chemical screening

Overnight culture of 2Δ or 5Δ cells in YPD was diluted with YPD medium to OD_{600} = 0.01 and its 40 μl aliquots were dispensed to the assay-ready 384-well plates with compounds using a liquid dispenser (MultiFlo FX, BioTek). After 24h incubation at 30°C, the 384-well plates were thoroughly vortexed using a MixMate (Eppendorf) and OD_{600} values were measured using a plate reader (Epoch 2, BioTek).

In vitro phospholipid synthesis/transport assays

The *in vitro* assay to monitor the fate of ^{14}C-labeled PS was performed essentially as described previously.[52,53] Briefly, [^{14}C(U)]-L-serine was added to yeast membrane fractions (12,000 × *g* pellet) resuspended in assay buffer (300 mM sucrose, 20 mM Tris-HCl, pH 7.5, 40 mM KCl, 2 mM CTP, 1 mM S-adenosylmethionine, 0.1 mM $MnCl_2$, 2 mM $MgCl_2$) at a final concentration of 2 μCi/ml. To observe PE methylation, we added ^{3}H-SAM to yeast membrane fractions (100,000 × *g* pellet) resuspended with the assay buffer (20 mM Tris-HCl pH 7.5, 300 mM Sucrose, 40 mM KCl, 2 mM CTP, 0.5 mM L-Serine, 0.1 mM $MnCl_2$, 2 mM $MgCl_2$) at a final concentration of 15 μCi/ml. To stop the reactions, we added 900 μl of 2:1 chloroform/methanol to the samples and vortexed for 15 min. Then, 200 μl of 0.1 M KCl/0.1 M HCl was added to the samples and further vortexed for 15 min at room temperature. After 5 min spin, the organic phase was collected and dried under N_2 gas. The resulting lipids were dissolved in chloroform and subjected to the analysis by thin-layer chromatography (TLC) followed by radioimaging with an Amersham Typhoon scanner.

Immunoblotting

For immunoblotting, proteins were transferred to polyvinylidene fluoride Immobilon-FL or Immobilon-P membranes (Millipore). The transferred proteins were detected by fluorophore-conjugated to secondary antibodies (Cy5 AffiniPure Goat Anti-Rabbit IgG (H+L), Jackson ImmunoResearch Laboratories) and analyzed with a Typhoon imager (GE Healthcare).

Fluorescence microscopy

Logarithmically growing yeast cells cultivated in SCD were observed using a model IX83 microscope (Olympus) with a CSU-X1 confocal unit (Yokogawa), a 100× and 1.4 numerical aperture objective lens (UPlanSApo; Olympus), and an EM-CCD camera (Evolve 512; Photometrics). MetaMorph software (Molecular Devices) was used to analyze images. GFP was excited using a 488-nm laser (OBIS; Coherent) and the emission was passed through 520/35-nm filter. The confocal fluorescent sections were collected every 0.2 μm from the upper to the bottom surface of yeast cells. The obtained confocal images were subjected to maximum projection using Image J software (NIH).

Membrane potential measurement

The membrane potential of mitochondria isolated from wild-type yeast cells grown in YPLac was measured using the fluorescent dye JC-1. Briefly, 400 μg mitochondrial fractions were resuspended in 100 μl assay buffer (600 mM mannitol, 20 mM HEPES-KOH pH 7.5, 40 mM KCl, 0.25% BSA, 5 mM ATP, 200 nM JC-1) with or without either 20 μM PCiB compound or 30 μM CCCP. Samples were incubated at 30°C for 30 min and fluorescence was measured at excitation/emission 485/535 and 535/595 nm. The mitochondrial membrane potential was expressed as the ratio of red to green fluorescence.

Chemicals

Chemical compounds for screening were obtained from the Drug Discovery Initiative at the University of Tokyo (Tokyo, Japan). PCiB-1 (Asinex), PCiB-2 (Enamine), PCiB-3 (Enamine), PCiB-4 (Vitas-M), PCiB-2 analog (Maybridge), PCiB-3 analog (Labotest), PCiB-4 analog (Enamine, Zelinsky Institute) were used from stock solutions of 100 mM in DMSO.

PCiB-1 analog was synthesized by the reaction of 2,4-difluorophenyl isocyanate with 3-((3-azido-5-(azidomethyl)benzyl)thio)-1,2,4-thiadiazol-5-amine (Figure S3). All reactions were performed with dry glassware under atmosphere of argon. Analytical thin-layer chromatography (TLC) was performed on precoated (0.25 mm) silica-gel plates (Merck Chemicals, Silica Gel 60 F254, Cat. No. 105715). Preparative thin-layer chromatography (PTLC) was performed on silica-gel (Wako Pure Chemical Industries Ltd., Wakogel B-5F, Cat. No. 230-00043). Melting point (Mp) was measured on an OptiMelt MPA100 (Stanford Research Systems) and is uncorrected. ^{1}H NMR spectra were obtained with a Bruker AVANCE 500 or 400 spectrometer at 500 or 400 MHz. ^{13}C NMR spectra were obtained with a Bruker AVANCE 500 or 400 spectrometer at 126 or 101 MHz. ^{19}F NMR spectrum was obtained with a Bruker AVANCE 400 spectrometer at 376 MHz. $CDCl_3$ (Kanto Chemical Co., Inc.,

Cat. No. 07663- 23) or DMSO-d_6 (Kanto Chemical Co., Inc., Cat. No.11560-43) was used as a solvent for obtaining NMR spectra. Chemical shifts (δ) are given in parts per million (ppm) downfield from $(CH_3)_4Si$ (δ 0.00 for ^{1}H NMR in $CDCl_3$) or the solvent peak (δ 77.0 for ^{13}C NMR in $CDCl_3$, δ 2.50 for ^{1}H NMR, and δ 39.5 for ^{13}C NMR in DMSO-d_6) as an internal reference or α,α,α-trifluorotoluene (δ –63.0 ppm for ^{19}F NMR in DMSO-d_6) as an external standard with coupling constants (*J*) in hertz (Hz). The abbreviations s, d, m, and br signify singlet, doublet, multiplet, and broad, respectively. IR spectra were measured by diffuse reflectance method on a Shimadzu IRPrestige-21 spectrometer attached with DRS-8000A with the absorption band given in cm^{-1}. High-resolution mass spectra (HRMS) were measured on a Bruker micrOTOF mass spectrometer under positive electrospray ionization (ESI^+). 3,3′-Disulfanediylbis(1,2,4-thiadiazol-5-amine)[87] and 1-azido-3-(azidomethyl)-5-(bromomethyl)benzene[88] were prepared by the reported method.

Characterization data of compounds

Synthesis of 3-((3-azido-5-(azidomethyl)benzyl)thio)-1,2,4-thiadiazol-5-amine (S1)

To a solution of 3,3′-disulfanediylbis(1,2,4-thiadiazol-5-amine) (78.8 mg, 247 μmol) in EtOH (7.0 mL) were added KOH (55.3 mg, 986 μmol, 4.0 equiv) and 1-azido-3-(azidomethyl)-5-(bromomethyl)benzene (66.0 mg, 247 μmol) dissolved in EtOH (0.50 mL) at room temperature. After stirring for 2 h at the same temperature, to the mixture was added H_2O. The mixture was extracted with CH_2Cl_2, and the combined organic extract was washed with brine, dried (Na_2SO_4), and after filtration, the filtrate was concentrated under reduced pressure. The residue was purified by preparative TLC (*n*-hexane/EtOAc = 1/1) to give **S1** (60.6 mg, 190 μmol, 77%) as a pale yellow oil. TLC R_f 0.62 (*n*-hexane/EtOAc = 1/1); ^{1}H NMR ($CDCl_3$, 500 MHz) δ 7.14 (s, 1H), 7.09 (s, 1H), 6.86 (s, 1H), 5.48–5.66 (br s, 2H), 4.37 (s, 2H), 4.32 (s, 2H); ^{13}C NMR ($CDCl_3$, 126 MHz) δ 182.7, 166.7, 140.8, 140.3, 137.6, 125.1, 119.4, 117.5, 54.2, 35.3; IR (KBr, cm^{-1}) 3396, 2112, 1607, 1518, 1250; HRMS (ESI^+) *m/z*: $[M + H]^+$ Calcd for $C_{10}H_{10}N_9S_2^+$ 320.0495; Found 320.0494 (Figure S4).

Synthesis of 1-(3-((3-azido-5-(azidomethyl)benzyl)thio)-1,2,4-thiadiazol-5-yl)-3-(2,4-difluorophenyl)urea (PCiB-1 analog)

To a solution of *S1* (38.7 mg, 121 μmol) in 1,4-dioxane (2.0 mL) were added 4-methylmorpholine (40.0 μL, 365 μmol, 3.0 equiv) and 2,4-difluorophenyl isocyanate (16.0 μL, 137 μmol, 1.1 equiv) at room temperature. After stirring with heating at 50°C for 24 h, the mixture was cooled to room temperature and concentrated under reduced pressure. The residue was purified by preparative TLC (*n*-hexane/acetone = 3/1) to give PCiB-1 analog (17.4 mg, 36.7 μmol, 30%) as a colorless solid. Mp 167 ºC (decomp.); TLC R_f 0.42 (*n*-hexane/acetone = 3/1); ^{1}H NMR (DMSO-d_6, 400 MHz) δ 11.42–11.74 (br s, 1H), 9.09 (s, 1H), 7.87–8.00 (m, 1H), 7.33–7.43 (m, 1H), 7.26 (s, 1H), 7.19 (s, 1H), 7.06–7.14 (m, 1H), 7.03 (s, 1H), 4.46 (s, 2H), 4.45 (s, 2H); ^{13}C NMR (DMSO-d_6, 101 MHz) δ 176.8, 164.7, 158.2 (dd, J_{C-F} = 245.0, 12.0 Hz), 153.3 (dd, J_{C-F} = 247.7, 12.9 Hz), 152.0, 140.6, 139.8, 138.0, 125.4, 123.7 (d, J_{C-F} = 8.4 Hz), 122.1 (dd, J_{C-F} = 11.3, 3.6 Hz), 119.1, 117.7, 111.4 (dd, J_{C-F} = 22.1, 3.4 Hz), 104.2 (dd, J_{C-F} = 27.1, 23.9 Hz), 52.8, 34.2; ^{19}F NMR (DMSO-d_6, 376 MHz) δ –117.0, –124.3; IR (KBr, cm^{-1}) 3385, 2106, 1719, 1545, 1229; HRMS (ESI^+) *m/z*: $[M + H]^+$ Calcd for $C_{17}H_{13}F_2N_{10}OS_2^+$ 475.0678; Found 475.0663 (Figure S4).

QUANTIFICATION AND STATISTICAL ANALYSIS

Data are shown as mean with standard error. Unpaired two-tailed student's t-test were performed for the statistical analyses using Prism 6 software (GraphPad). IC50 values were calculated using Prism 6 software (GraphPad).